Chem Soc Rev

REVIEW ARTICLE

View Article Online
View Journal | View Issue

Cite this: *Chem. Soc. Rev.*, 2024, **53**, 9560

Transition-metal-catalyzed enantioselective C–N cross-coupling

Jia Feng,[a] Long-Long Xi,[a] Chuan-Jun Lu [a] and Ren-Rong Liu *[abc]

Chiral amine scaffolds are among the most important building blocks in natural products, drug molecules, and functional materials, which have prompted chemists to focus more on their synthesis. Among the accomplishments in chiral amine synthesis, transition-metal-catalyzed enantioselective C–N cross-coupling is considered one of the most efficient protocols. This approach combines traditional C(sp^2)–N cross-coupling methods (such as the Buchwald–Hartwig reaction Ullmann-type reaction, and Chan–Evans–Lam reaction), aryliodonium salt chemistry and radical chemistry, providing an attractive pathway to a wide range of structurally diverse chiral amines with high enantioselectivity. This review summarizes the established protocols and offers a comprehensive outlook on the promising enantioselective C–N cross-coupling reaction.

Received 31st January 2024

DOI: 10.1039/d4cs00102h

rsc.li/chem-soc-rev

1. Introduction

C–N coupling is considered one of the most important transformations in organic synthesis, producing alkyl/aryl amines that serve as the foundational structures for natural products, pharmaceuticals, drug candidates, and other bioactive molecules (Scheme 1a).[1] Dating back to 1903, Ullmann pioneered the copper-catalyzed C–N coupling for the synthesis of aryl amines from aryl chlorides and anilines.[2] For more practical and efficient approaches to producing aryl amines, Buchwald and Hartwig independently developed palladium-catalyzed C–N couplings in 1995.[3,4] With the rise of chiral chemistry, chiral amines have become essential and promising components in chiral catalysts and drugs.[4–6] As a result, significant efforts have been dedicated to the development of enantioselective synthesis of chiral amines, with enantioselective C–N coupling being regarded as one of the most important and powerful tools.

Along with the rapid development of Ullmann-type C–N coupling, its enantioselective variant has been successfully used to synthesize chiral arylamines.[7] The screening of optimal copper salts and ligands has enabled the production of chiral amines under mild conditions, thus overcoming the drawbacks

[a] *College of Chemistry and Chemical Engineering, Qingdao University, Ningxia Road 308#, Qingdao 266071, China. E-mail: renrongliu@qdu.edu.cn*
[b] *Key Laboratory of Shandong Provincial Universities for Functional Molecules and Materials, Qingdao University, Qingdao 266071, China*
[c] *College of Pharmaceutical Sciences, Guizhou University, Guiyang, 550025, China*

Jia Feng

Prof. Jia Feng received his PhD degree from the University of Science and Technology of China (USTC) under the supervision of Prof. Zhenhua Gu in 2018. From 2018 to 2022, he worked as a postdoctoral fellow and an associate research fellow at USTC. In 2022, he moved to Qingdao University as an associate professor. His current research interest is transition-metal-mediated asymmetric catalysis.

Long-Long Xi

Prof. Long-Long Xi was born in Shaanxi province, People's Republic of China, in 1995. He received his BS degree in chemistry with Prof. Bao-Xiang Zhao from Shandong University in 2018. Then, he moved to Nanjing University and completed his PhD in organic chemistry with Prof. Zhuangzhi Shi. In 2023, he joined the faculty at Qingdao University. His current research efforts are focused on synthetic methodology, including asymmetric catalysis, transition-metal catalysis and the activation of inert chemical bonds.

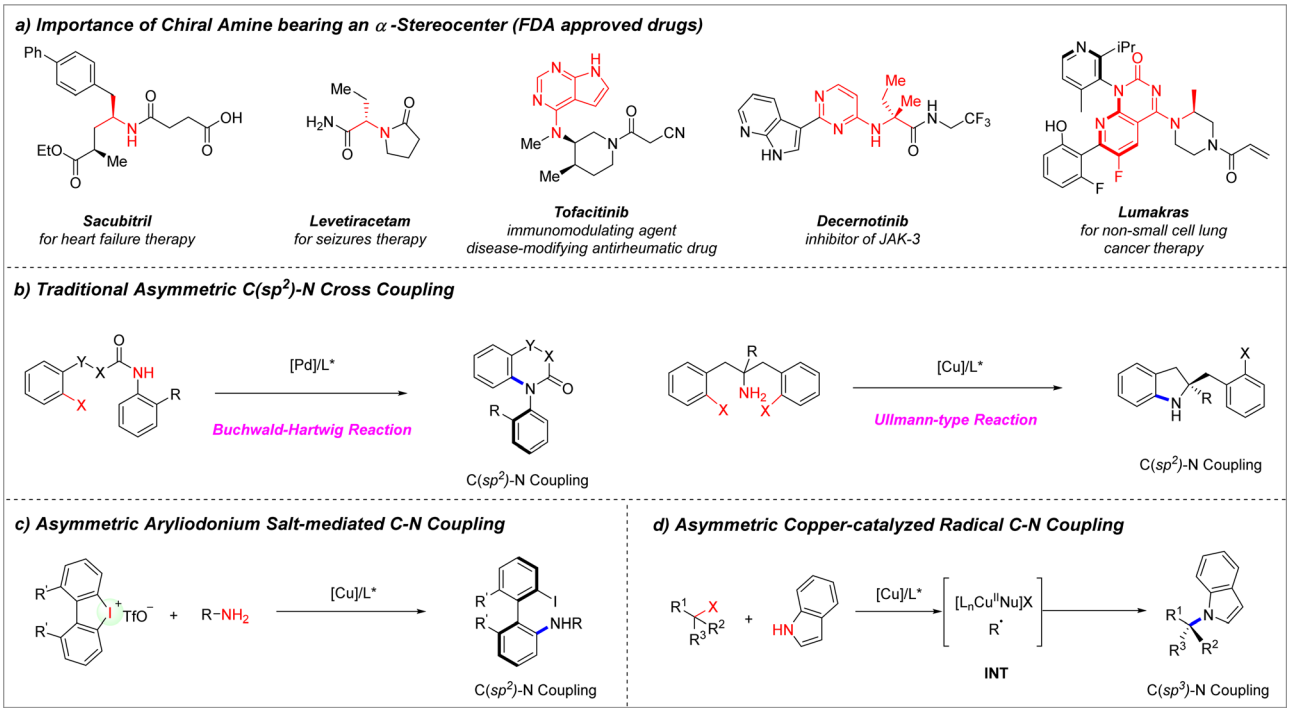

Scheme 1 (a) Representative chiral amines bearing an α-stereocenter; (b) traditional asymmetric C(sp^2)–N cross-coupling; (c) asymmetric aryliodonium salt-mediated C–N coupling; (d) asymmetric copper-catalyzed radical C–N coupling.

of the harsh reaction conditions (high temperatures) associated with traditional Ullmann C–N couplings. Additionally, intramolecular C–N coupling is crucial for achieving excellent enantioselectivity in most cases of enantioselective synthesis. Another traditional coupling, the Buchwald–Hartwig reaction, has emerged as a powerful tool for constructing chirality in recent decades. Leveraging structurally diverse phosphine ligands, the Buchwald–Hartwig amination offers greater possibilities for achieving perfect stereocontrol.[8] Both Ullmann-type C–N coupling and the Buchwald–Hartwig reaction lead to the production of chiral arylamines, thus contributing to enantioselective synthesis and functional research in this important scaffold (Scheme 1b).

Hypervalent iodine(III) compounds are extensively explored and valuable synthons due to their convenient accessibility and excellent reactivity.[9,10] Among various hypervalent iodine salts, diaryliodonium salts with strong electrophilic properties serve as suitable surrogates for aryl halides, which are often used as coupling partners in copper-catalyzed enantioselective C–N couplings.[11] For acyclic diaryliodoniums, C–N atropisomers are synthesized by connecting *ortho*-substituted aryl moieties and amines. In 2018, Colobert and Wencel-Delord pioneered the first synthesis of C–N atropisomers through copper-catalyzed C–N coupling.[12] When cyclic diaryliodoniums were employed in the enantioselective C–N coupling, excellent

Chuan-Jun Lu

Dr Chuan-Jun Lu received her PhD degree from Sun Yat-sen University in 2013. She is currently a lecturer at Qingdao University. Her current research interests focus on transition-metal-mediated asymmetric catalysis and pharmaceutical chemistry.

Ren-Rong Liu

Prof. Ren-Rong Liu received his PhD degree from East China Normal University under the supervision of Prof. Junliang Zhang in 2013. From 2013 to 2018, he worked at Zhejiang University of Technology. After working as a postdoctoral fellow with Prof. Andy McNally at Colorado State University, he became a professor at Qingdao University in 2019. His research interests include transition-metal-catalyzed synthetic methodologies and asymmetric synthesis.

reaction efficiency was achieved by forming a C–N bond to yield aryl iodides.[13] In 2018, Hayashi conducted an early trial of the copper-catalyzed enantioselective C–N coupling process using cyclic diaryliodonium salts.[14] The use of diaryliodonium salts as mediators in enantioselective C–N couplings has seen significant advancements in the last decade, significantly expanding the versatility of this type of coupling (Scheme 1c).

Radicals are widely known to be highly reactive and unstable, making the ability to harness them in enantioselective synthesis both highly desirable and challenging. Significant progress has recently been achieved by combining copper catalysis with radical chemistry for enantioselective C–N coupling, enabling the access to chiral alkyl amines.[15] A groundbreaking study by Fu in 2016 demonstrated the feasibility of copper-catalyzed enantioselective C–N coupling through a radical process with the aid of visible light.[16] Since then, giant leaps have been made in the field of radical-mediated enantioselective C–N coupling (Scheme 1d).

This review will focus on three main aspects related to enantioselective C–N coupling: (1) traditional enantioselective C(sp^2)–N cross coupling; (2) C(sp^2)–N cross coupling mediated by diaryliodonium salts; and (3) enantioselective C(sp^3)–N cross coupling involving radicals. Other remarkable developments in the synthesis of chiral amines such as reductive enantioselective amination of ketones/hydrides,[17,18] enantioselective allylic amination,[19,20] enantioselective hydroamination of alkenes,[21] enantioselective amination of non-acidic C(sp^3)–H bonds,[22] Pd-catalyzed enantioselective cyclization reactions,[23] enantioselective carbene insertion into N–H bonds,[24,25] and palladium/norbornene mediated tandem enantioselective C–N coupling reactions,[26,27] among others, will not be covered in this review.

2. Traditional enantioselective C(sp^2)–N cross-coupling

Over the past few decades, traditional C(sp^2)–N cross-couplings, namely the Buchwald–Hartwig reaction and the Ullmann reaction, have emerged as powerful tools for forging C(sp^2)–N bonds. This is of vital importance to the pharmaceuticals, materials, and catalysis fields. However, their enantioselective variants are still in their infancy owing to limited chiral types and slow progress in ligand design. Whether it is enantioselective Buchwald–Hartwig coupling or enantioselective Ullmann-type C–N coupling, both heavily rely on ligand design. The last few decades have witnessed a rapid evolution in chiral ligands, which has contributed to the surge in enantioselective C(sp^2)–N cross-coupling. This section will provide an overview of reported enantioselective Buchwald–Hartwig coupling, enantioselective Ullmann-type C–N coupling, and other transition-metal-mediated C–N coupling systems.

2.1 Enantioselective Buchwald–Hartwig reaction

With the continual development of chiral catalysts, including structurally diverse phosphine ligands, the enantioselective Buchwald–Hartwig coupling has seen significant advancements in recent decades.[28] In 1997, Pye and Rossen pioneered the enantioselective Buchwald–Hartwig coupling through a kinetic resolution of *rac*-4,12-dibromo[2.2]paracyclophane **1** with benzyl amine (Scheme 2).[29] The enantioselective amination proceeded smoothly with 4,12-bis(diphenylphosphino)[2.2]-paracyclophane **L1** as the ligand, resulting in chiral arylamine **2** and leaving behind **1** with up to 93% enantiomeric excess (ee) and 42% resolution conversion. The efficiency of this protocol was demonstrated through the synthesis of chiral phosphine ligand **L1** using the obtained enantioenriched **1** as starting materials, providing a pathway to access planar bisphosphines.

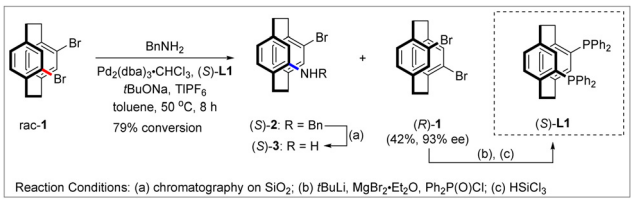

Scheme 2 Early research on enantioselective Buchwald–Hartwig reaction.

2.1.1 Enantioselective coupling with alkyl amines. In 2015, Bräse reported a diastereoselective synthesis of amines **6** from racemic bromide **4** and chiral 1-phenylethan-1-amine **5** (Scheme 3a).[30] Both ligands such as Taniaphos **L2** or racemic BINAP were utilized, resulting in up to 91% diastereoselectivity. A similar procedure was carried out by Ohta to obtain enantioenriched aryl amines through enantioselective Buchwald–Hartwig amination (Scheme 3b).[31] The catalysis of palladium and chiral ligand (*R*)-Tol-BINAP facilitated the enantioselective C–N coupling, leading to the successful formation of chiral amine **9** with moderate to good enantioselectivity. Control experiments indicated that aryl iodides were better coupling partners compared to bromides under the reaction conditions, resulting in higher enantioselectivity of the product.

2.1.2 Enantioselective coupling with aryl amines. In comparison to alkyl amines, aryl amines with moderate reactivities proved to be suitable counterparts in the asymmetric Buchwald–Hartwig reaction. In 1998, Kočovský and Vyskočil

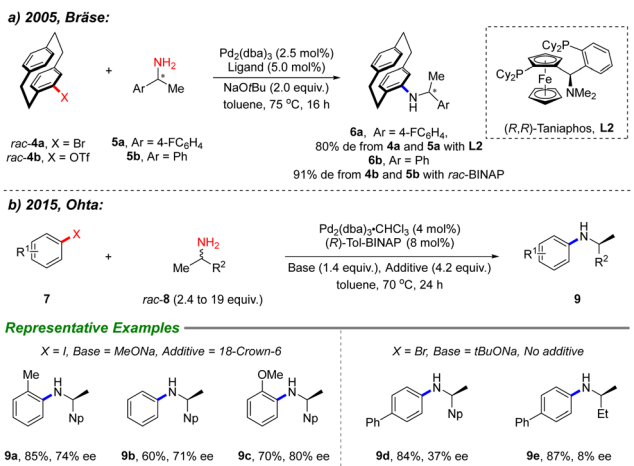

Scheme 3 Enantioselective C–N amination with alkyl amines.

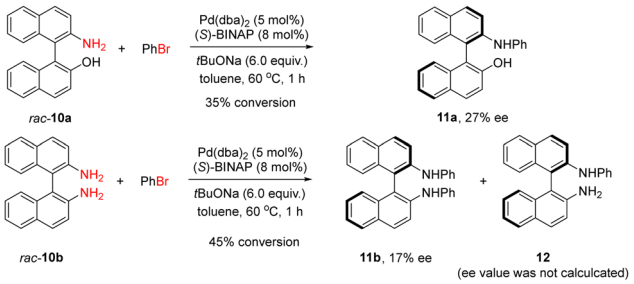

Scheme 4 Primary research on enantioselective C–N amination on kinetic resolution.

attempted the kinetic resolution of naphthyl amine and binaphthyl diamine through enantioselective C–N couplings (Scheme 4).[32] The primary results indicated that the enantioselective amination proceeded with the racemic **10a** as the substrate, yielding an arylation product with 35% conversion and 27% enantioselectivity. When naphthyl diamine **10b** was used, diarylation occurred to deliver **11b** with 17% ee. Although lowering the temperature could potentially improve the efficiency of the kinetic resolution, the relatively low solubility of **10a** or **10b** in toluene at lower temperatures hindered its enhancement.

In 2016, Lassaletta and Fernández reported an N,P-ligand QUINAP **L3**-mediated enantioselective synthesis of atropisomers through the enantioselective C–N amination of aryl bromides **13** and arylamines (Scheme 5).[33] To shed light into the stereocontrol process, X-ray diffraction analysis of a single crystal of the intermediate derived from the oxidative addition of aryl bromide and palladium was conducted. The angles of [C1′–C1–C10] and [C1–C1′–C10′] were found to be significantly greater than the normal 120° angle (127.6° and 125°, respectively), indicating a distorted configuration. This result confirmed that the oxidative addition was the stereo-determining step, making the enantioselective C–N amination a dynamic kinetic resolution process. With the assistance of palladium and chiral QUINAP, the enantioselective C–N amination proceeded smoothly to afford the atropisomeric amines **14** with excellent yields and enantioselectivities.

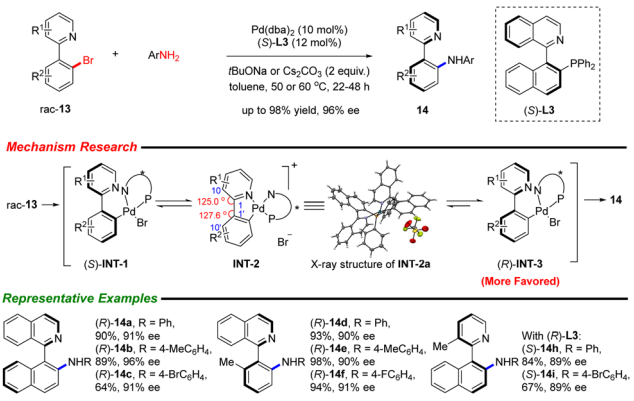

Scheme 5 QUINAP-mediated enantioselective C–N coupling.

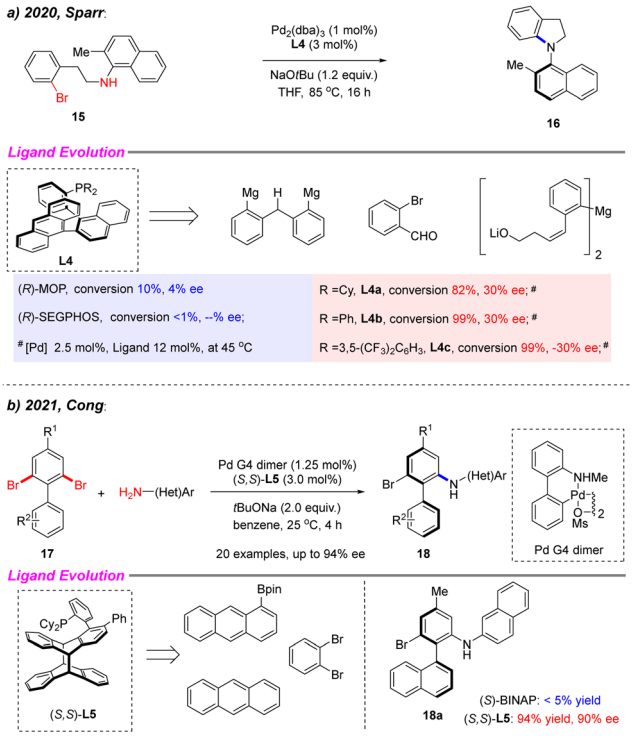

Scheme 6 Ligand evolution in enantioselective C–N couplings.

The evaluation of the ligand in enantioselective Buchwald–Hartwig amination is of vital importance for broadening its application in enantioselective synthesis.[8] In 2020, Sparr reported the synthesis of the chiral monophosphine ligand **L4** bearing an anthracenyl group, which was used in enantioselective C–N couplings (Scheme 6a).[34] The synthetic procedure for **L4** involved an enantioselective aldol condensation and a direct ester-to-anthracene transfer. The efficiency of **L4** was evaluated through intramolecular C–N amination, demonstrating superior stereo-inducing capabilities compared to the commercially available ligands MOP and SEGPHOS. Subsequently, Cong described the synthesis of chiral monophosphine ligand **L5**, which possessed a rigid scaffold and dual chirality, for use in the intermolecular enantioselective Buchwald–Hartwig reaction (Scheme 6b).[35] The synthetic route included a [4+4] photocycloaddition of borylated anthracene and anthracene, allowing the synthesis of diverse-substituted ligands. Under the reaction conditions, **L5** was found to be superior to the traditional ligand BINAP (resulting in $<5\%$ *versus* 94% yield with 90% ee). With the aid of palladium and the newly developed ligand **L5**, a series of atropisomeric arylamines were obtained with up to 94% ee.

In 2020, Wang and Tong successfully achieved an intramolecular enantioselective C–N coupling to produce inherently chiral ABCD-type heteracalix[4]aromatics (Scheme 7).[36] With the catalysis of palladium/JOSIPHOS, the intramolecular cyclization proceeded smoothly to deliver inherently chiral **20** with up to $>99\%$ ee. This approach offered a feasible avenue to access enantioenriched heteracalix[4]aromatics, which are typically challenging to prepare through catalytic enantioselective

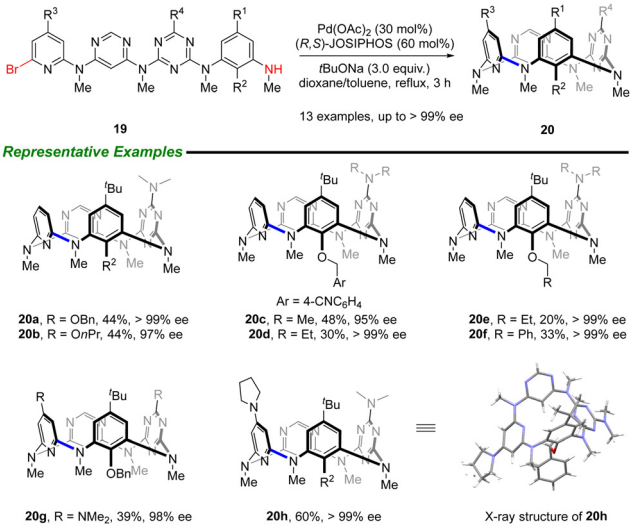

Scheme 7 Enantioselective C–N couplings for inherently chiral heteracalix[4]aromatic synthesis.

synthesis. The stereo-induced process was attributed to the *N*-nucleophilic approach of the palladium/ligand intermediates. The resulting enantiopure heteracalix[4]aromatics exhibited remarkable circularly polarized luminescence properties, suggesting promising potential applications in the field.

By using large steric hindrance of electron-rich arylphosphine ligands, aryl chlorides could be utilized in the asymmetric Buchwald–Hartwig reaction. In 2023, Zhu and Gandon reported the enantioselective intermolecular C–N cross-coupling for the construction of quaternary carbon stereocenters using a desymmetrization strategy (Scheme 8).[37] The key to their success was the use of the amino acid-derived ionic chiral ligand **L6**. With the aid of **L6**, the coupling products **22** were achieved with up to 99% ee. These results demonstrate excellent stereocontrol at the distal position of the chiral center of the substituents, which may have promising applications in asymmetric synthesis.

2.1.3 Enantioselective coupling with amides. Amides are common reaction counterparts in enantioselective Buchwald–Hartwig reactions. In 2009, Sasai reported the first enantioselective synthesis of chiral spiranes through a double C–N coupling process (Scheme 9a).[38] The chirality originated from

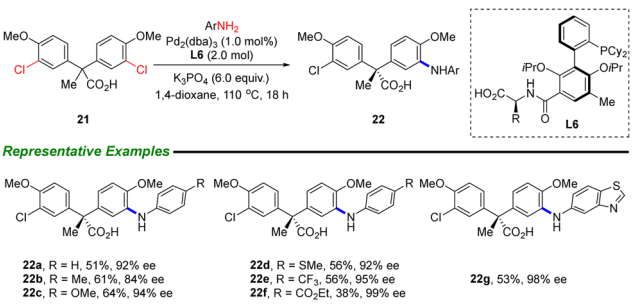

Scheme 8 Enantioselective intermolecular C–N coupling assisted with amino acid-derived ionic chiral ligand.

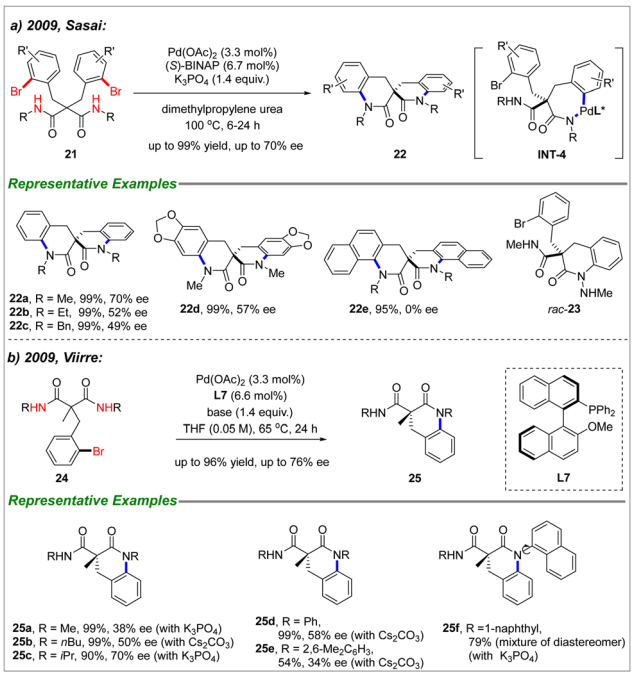

Scheme 9 Desymmetrization strategy in enantioselective Buchwald–Hartwig amination.

the intermediate **INT-4**, which was formed during the first C–N amination step. When *rac*-**23** was used as the substrate under standard conditions, both the cyclized product and the remaining starting material were racemic. By using $Pd(OAc)_2$/(*S*)-BINAP as the catalyst, a series of chiral spiranes were successfully obtained with moderate to good enantioselectivities. In the same year, Viirre reported the enantioselective intramolecular Buchwald–Hartwig amination of α-(2-bromobenzyl)-malonamides **24** *via* a desymmetrization process (Scheme 9b).[39] With the assistance of chiral ligand MOP **L7**, the enantioselective synthesis proceeded smoothly to produce the cyclized product **25** with moderate to good enantioselectivity. Notably, when the substituent was a 1-naphthyl group, a chiral axis was formed, leading to the formation of a product (**25f**) with central chirality.

Proceeding with intermolecular asymmetric Buchwald–Hartwig reactions presents greater challenges compared to intramolecular reactions. In 2005, Taguchi introduced the enantioselective intermolecular Buchwald–Hartwig reaction, leading to the formation of C–N atropisomers (Scheme 10).[40] With the aid of (*R*)-DTBM-SEGPHOS, the enantioselective *N*-arylation of *ortho*-substituted aryl amides **26** yielded **27** with up to 94% ee. This protocol offers a new route to access enantioenriched atropisomeric anilides bearing a chiral C–N axis, representing the first practical enantioselective *N*-arylation. Subsequent investigations focused on the stability and configuration, aided by NMR spectroscopy.[41] The *E*/*Z* ratio was determined to be $>50:1$, indicating that *E*-rotamer was the major configuration. The authors proposed that the n–π repulsion between the phenyl group and the carbonyl group, as well as the steric repulsion between the ethyl group and the hydrogen atom influenced the observed configuration.

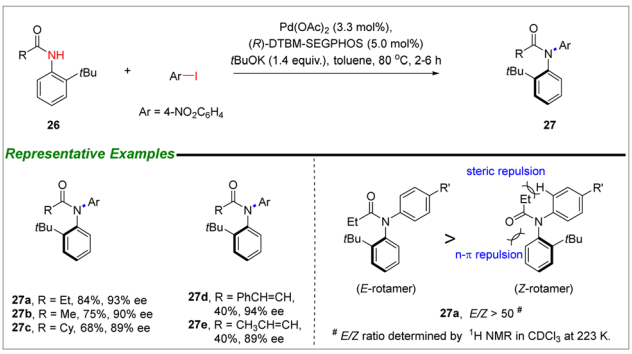

Scheme 10 Enantioselective intermolecular Buchwald–Hartwig amination.

Later, several research groups focused on the enantioselective synthesis of C–N atropisomers through intramolecular Buchwald–Hartwig amination. Kitagawa successfully achieved enantioselective intramolecular *N*-arylation of *ortho-tert*-butyl NH-anilides **28** in the presence of palladium and (*R*)-DTBM-SEGPHOS (Scheme 11a).[42] A series of lactams bearing a C–N axis were obtained with moderate to excellent enantioselectivities, and their ee values could be further increased through medium-pressure liquid chromatography (MPLC). The key intermediate **30** of the norepinephrine transporter (NET) inhibitor **31** was obtained with high enantioselectivity from the obtained **29a** through subsequent alkylation/allylation processes, highlighting the usefulness of this protocol.

In 2015, Nakazaki reported an enantioselective cyclization to access axially chiral aryloxindoles **33** *via* C–N coupling (Scheme 11b).[43] By using **L8** as the stereo-inducing source, **33** was obtained in 72% yield with 81% ee. Subsequent bromination and hydrolysis converted **33** to *N*-arylisatin **34**. Addition of MeLi resulted in **35** diastereoselectively (95 : 5 d.r.). The final step involved the removal of the aryl group to produce 3-hydroxy-3-metheyloxindole **36** with 81% ee. This chemistry provides a practical synthesis route for C–N atropisomers bearing the aryloxindole scaffold.

Later, Kitagawa accomplished the enantioselective synthesis of phenanthridin-6-one derivatives bearing a C–N axis through intramolecular C–N couplings (Scheme 11c).[44] The catalyst system, which includes $Pd(OAc)_2$/(*R*)-DTBM-SEGPHOS, facilitated the efficient synthesis of C–N atropisomers **38** with up to 77% ee. Detailed research revealed that factors such as the choice of base, solvents, reaction temperature, and the substituent at the *ortho* position of the substrates significantly impacted the enantioselectivity.

The synthesis of the above-mentioned C–N atropisomers is constrained by relatively narrow substrate scopes or limited stereo-control efficiency (Schemes 6, 10 and 11). Recently, Li successfully achieved the intermolecular Buchwald–Hartwig reaction for the synthesis of C–N atropisomers through the de devo synthesis of the C–N axis (Scheme 12).[45] With the aid of chiral ligand **L9**, the enantioselective C–N coupling proceeded smoothly to deliver C–N atropisomers with diverse functional groups and excellent enantioselectivities. Control experiments were carried out using different *ortho*-substituted substrates, revealing that substrates with greater steric hindrance exhibited enhanced reactivity. With the help of DFT calculations, the

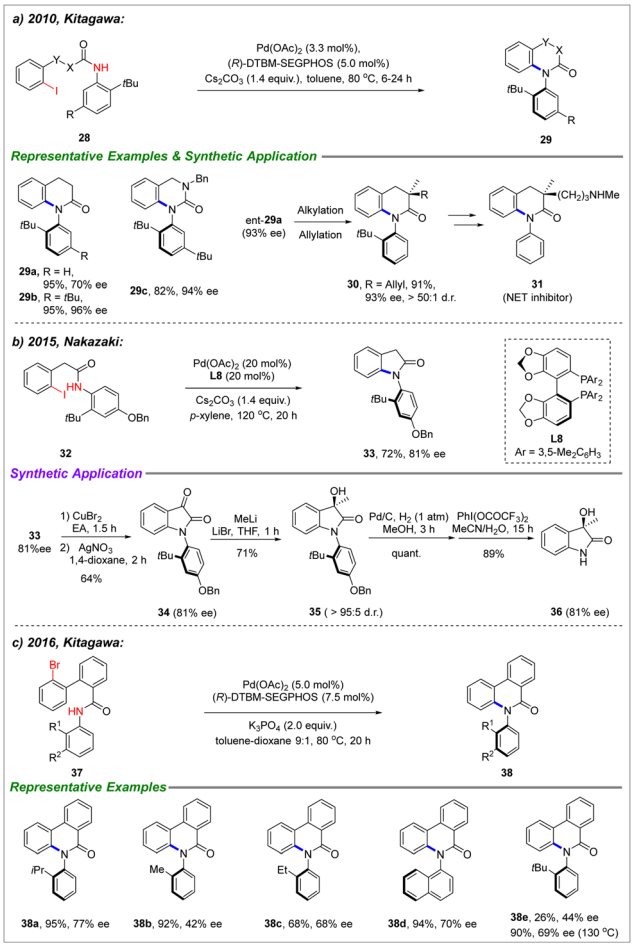

Scheme 11 C–N atropisomer synthesis *via* enantioselective cyclization.

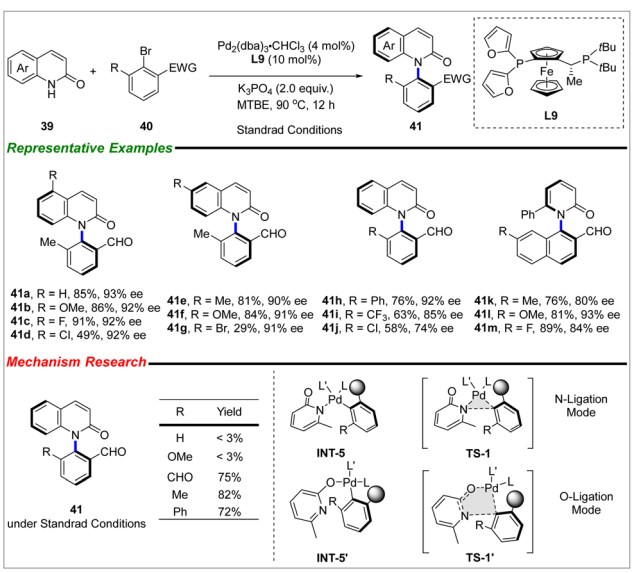

Scheme 12 Intermolecular enantioselective Buchwald–Hartwig reaction.

authors proposed an unusual O-ligation mode a five-member cycle in the transition state **TS-1′** as being more desirable compared to the N-ligation bearing a five-member cycle in **TS-1**.

2.1.4 Enantioselective coupling with other nitrogen sources. Other reactants with N-containing functional groups have also been applied in the enantioselective Buchwald–Hartwig reaction, leading to the formation of products with central or axial chirality and excellent enantioselectivities.

Enaminones can be used directly or can be formed *in situ* from amines and ynones in the enantioselective intramolecular Buchwald–Hartwig amination process. In 2012, Kitagawa reported the enantioselective cyclization of ynones **42** and anilines **43** in the presence of palladium and the chiral ligand MOP (Scheme 13a).[46] This tandem amination involved the 1,4-addition of **43** to **42**, followed by enantioselective C–N couplings. Eight representative examples were presented with up to 72% ee.

Recently, Knipe reported the enantioselective C–N coupling using enaminones **45** as the substrates directly (Scheme 13b).[47] Under the catalysis of $Pd(OAc)_2$/(*R*)-BINAP, a series of atropisomeric 4-quinolinones **44** were obtained with moderate enantioselectivities. The newly obtained products **44** could be further transformed into *N*-aryl quinolinium salts **46** with minimal loss of enantioselectivities. The structure of quinolinium salts was confirmed by X-ray diffraction of their single crystals. Using DFT, UV-vis, and racemization experiments, a high rotational barrier (~51 kcal mol^{-1}) and their solvatochromic behavior were confirmed. Recently, Qiu achieved enantioselective cyclization *via* C–N coupling with the aid of chiral ferrocene bisphosphine **L10**, yielding the desired products **44** with excellent yields and enantioselectivities (Scheme 13c).[48]

With enamines as substrates, the asymmetric synthesis could be applied to indole-based C–N atropisomer synthesis. In 2023, Liu, Parton, and Li presented an efficient enantioselective intramolecular *N*-arylation for the synthesis of C–N atropisomers (Scheme 14).[49] Under the catalysis of palladium and (*S*)-BINAP, a series of 4-quinolone atropisomers were successfully obtained with good to excellent enantioselectivities. The protocol could be extended to the enantioselective synthesis of indole-derived C–N atropisomers, yielding cyclized products **48** with excellent enantioselectivities. Notably, enantioenriched C–N atropisomers bearing two axes could be obtained through the enantioselective C–N coupling, which have potential applications as hole-transport materials.

In 2015, Li and Belyk reported the synthesis of chiral hemiaminal through an enantioselective Buchwald–Hartwig reaction (Scheme 15).[50] Under the reaction conditions, **49** underwent rapid racemization by transforming to the ring-opening substrate **49′**. Subsequently, a dynamic kinetic resolution procedure was successfully achieved by capturing one enantiomer with the aid of palladium and **L11**. This protocol demonstrated excellent functional group tolerance and enantioselectivity. The effectiveness of the protocol was further illustrated by its application in the enantioselective synthesis of elbasvir, a drug candidate for hepatitis C virus (HCV).

In 2022, Liu and Li reported the enantioselective synthesis of N–N atropisomers *via* a cascade condensation/C–N coupling process (Scheme 16).[51] Starting with α-aryl-ketoester **51** and

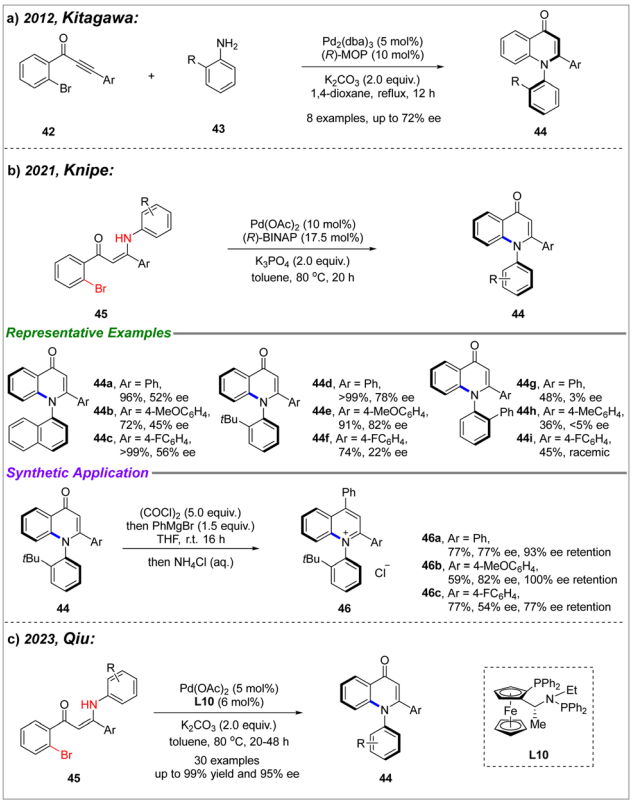

Scheme 13 Enantioselective Buchwald–Hartwig amination with enaminones.

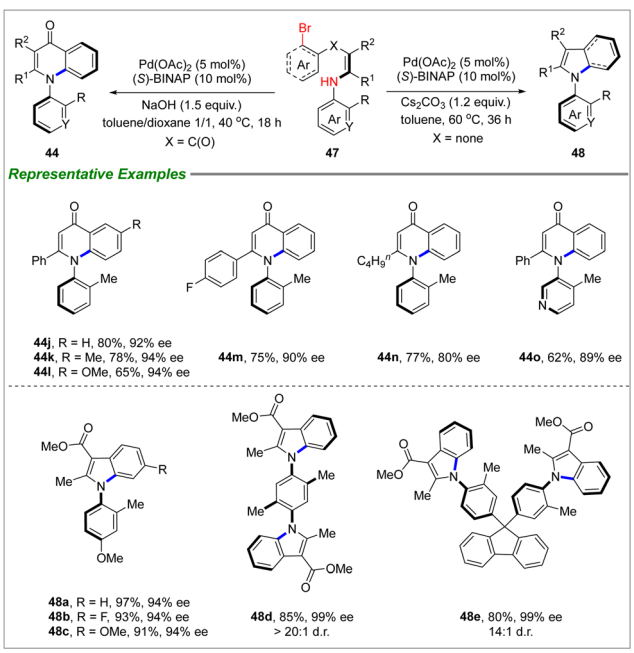

Scheme 14 Enantioselective Buchwald–Hartwig reaction for C–N atropisomer synthesis.

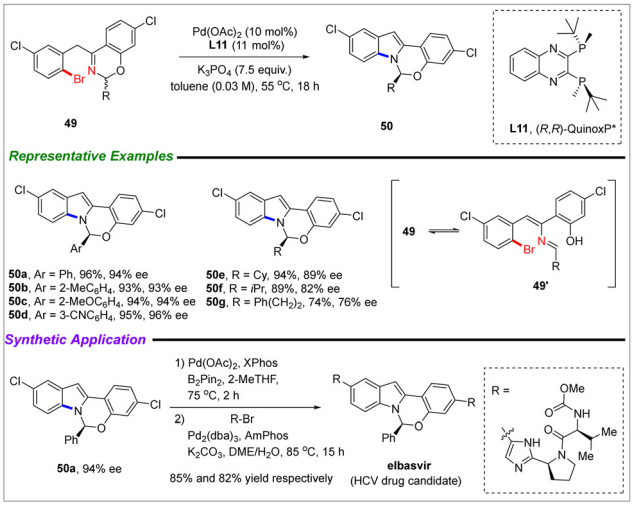

Scheme 15 Enantioselective Buchwald–Hartwig reaction for chiral hemiaminal synthesis.

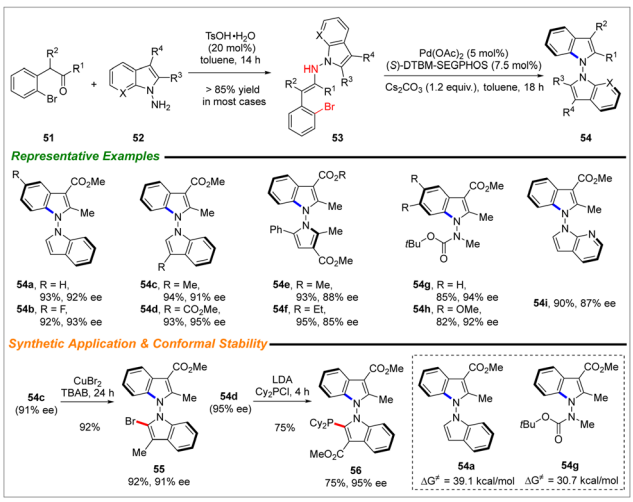

Scheme 16 Enantioselective tandem condensation/C–N couplings for N–N atropisomer synthesis.

amino indoles **52** as substrates, the two-step enantioselective synthesis featured C–N amination as the stereo-determining step using $Pd(OAc)_2$/(*S*)-DTBM-SEGPHOS as a catalyst. A variety of substrates were used, resulting in the formation of axially chiral N–N indole–indole, N–N indole–pyrrole, and indole–nonaryl atropisomers with excellent yields and enantioselectivities. The utility of this method was demonstrated by the successful synthesis of bromide **55** without any loss of enantioselectivity. The resulting N–N atropisomer was further utilized in the synthesis of axially chiral monophosphine **56** through the directed phosphinization of **54d**. Additionally, the stability of the chiral N–N axis was investigated through racemization experiments, revealing a relatively high rotational barrier ($\sim$39 kcal mol^{-1}) for this type of N–N atropisomer.

Substituted amidines could serve as suitable coupling partners in the enantioselective Buchwald–Hartwig reaction for the

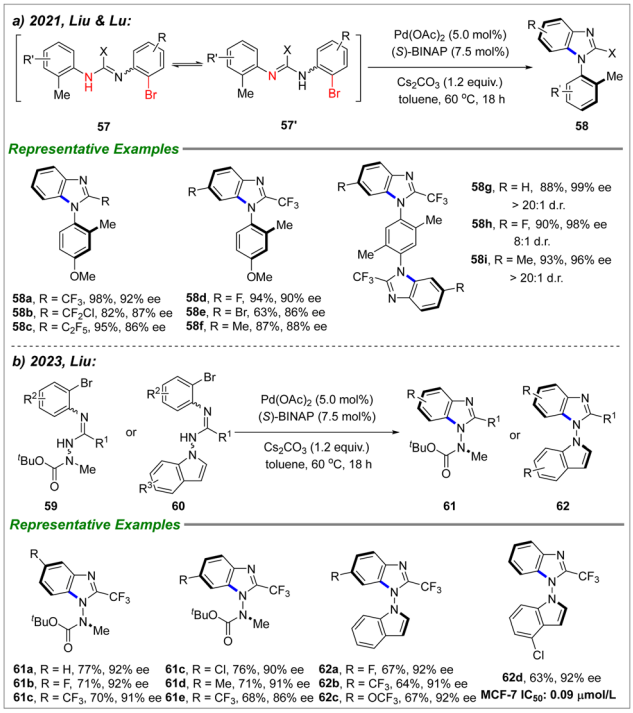

Scheme 17 Enantioselective Buchwald–Hartwig reaction of amidines.

construction of atropisomers with an aza axis. In 2021, Liu and Lu successfully achieved intramolecular C–N couplings of aryl amidines **57** for the synthesis of C–N atropisomers (Scheme 17a).[52] Under the reaction conditions, aryl amidines **57** underwent racemization by transforming into **57′**, and this equilibration was used to facilitate a dynamic kinetic resolution process for the synthesis of C–N atropisomers. A variety of functional C–N aryl-benzimidazole atropisomers were produced with high yields and excellent enantioselectivities. Notably, 1,4-dibenzimidazoles aryls bearing two C–N axes could be achieved using this methodology.

Based on a similar strategy, Liu reported the enantioselective C–N coupling of amidines **59** or **60** for the synthesis of N–N atropisomers (Scheme 17b).[53] With the aid of $Pd(OAc)_2$/(*S*)-BINAP, a wide range of N–N indole–benzimidazole or N–N indole–nonaryl atropisomers were successfully synthesized with excellent enantioselectivities. The potential application of the newly developed N–N atropisomeric moiety was examined through bioactive experiments, revealing that **62d** exhibited outstanding antitumor activity against the MCF-7 cell line (IC_{50}: 0.09 μmol L^{-1}).

2.2 Enantioselective Ullmann C–N coupling

The copper-catalyzed Ullmann-type C–N coupling has developed into a classic and efficient approach to construct C–N bonds.[54–56] However, the drawbacks of this type of coupling, such as high reaction temperatures and the need for stoichiometric amounts of copper, have hampered its wide application in industry and enantioselective synthesis. Recently, enantioselective Ullmann reactions have been achieved through the evolution of ligands. In 2006, Ma pioneered the first catalytic

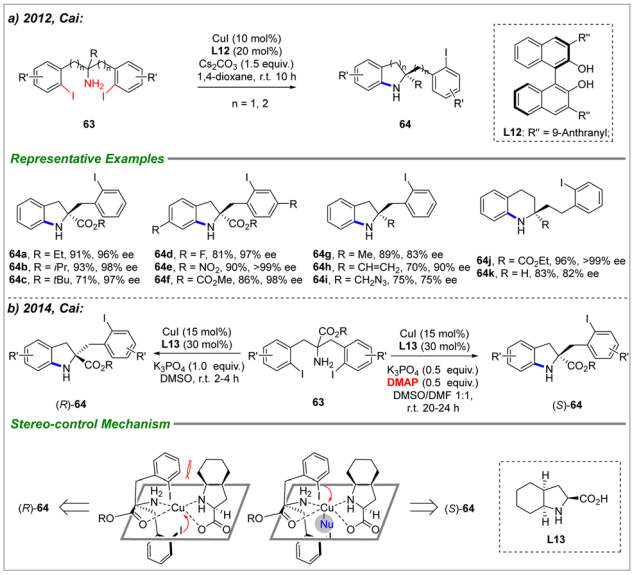

Scheme 18 Enantioselective intramolecular Ullmann C–N couplings.

enantioselective Ullmann type coupling.[57] Subsequently, a couple of research studies have been reported to construct central or axial chirality. This reaction can be divided into two main types: intramolecular coupling and intermolecular coupling in enantioselective synthesis.

2.2.1 Intramolecular coupling. In 2012, Cai developed the first enantioselective Ulmann-type C–N coupling for the synthesis of chiral indolines **63** (Scheme 18a).[58] Under the catalysis of CuI/BINOL-derived chiral ligand **L12**, a series of divergent functional indolines **64** were synthesized with excellent yields and enantioselectivities through enantioselective cyclization. The CuI/chiral amino acid **L13** system was found to be suitable for this type of enantioselective C–N coupling (Scheme 18b).[59] Subsequent research revealed that cyclized products **64** could be obtained with inversed enantioselectivities upon the addition of DMAP. A possible stereocontrol mechanism shed light on the enantioselective synthesis process. In the absence of the nucleophile DMAP, copper coordinated with substrates **63** and chiral ligand **L13** to form a planar intermediate. Then the attack of iodine and copper occurred at the bottom position due to steric interactions with the phenyl group and **L13**. With copper occupied by DMAP, a reversed configuration was obtained, with the attack of iodine to copper occurring at the upper position.

In 2014, Cai reported an enantioselective C–N amination for constructing an all-carbon quaternary stereocenter (Scheme 19).[60] Utilizing CuI/**L12** as the catalyst, the enantioselective cyclization proceeded smoothly to deliver **66** bearing a cyano group with excellent yields and enantioselectivities. After simple recrystallization, the optically pure coupling products could be obtained (**66i**). The utility of this protocol was demonstrated through the divergent transformation of the cyano moiety. By reducing the cyano group to an amino group, a second C–N coupling reaction was carried out to generate spiro-scaffold **67** with 100% enantioselectivity. Subsequent hydrolysis

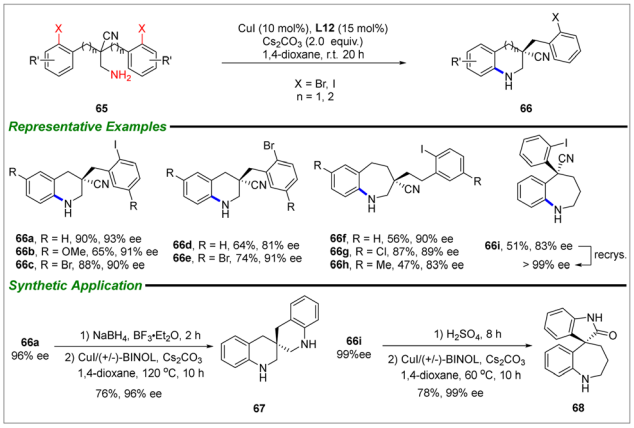

Scheme 19 Enantioselective Ullmann reaction to construct all-carbon quaternary stereocenter.

of the cyano group allowed for intramolecular C–N couplings of amides and amino groups, leading to the cyclized product **68** without compromising the enantioselectivity.

In 2013, Cai achieved an enantioselective C–N amination-based kinetic resolution (Scheme 20a).[61] Under CuI/**L12** catalysis, this process smoothly resolved *rac*-2-amino-3-(2-iodoaryl)-propionates or *rac*-2-amino-4-(2-iodoaryl)butanoates **69** to provide enantioenriched **69** and C–N coupling products **70** with excellent selectivity (*s* factor ~165). This marked the first application of copper-catalyzed C–N amination to a kinetic resolution process, offering an efficient route to chiral indolines. Subsequently, the same group extended the kinetic resolution approach to the synthesis of chiral indolines bearing a quaternary stereocenter at the β-position of the N atom (Scheme 20b).[62]

In 2015, Cai developed a method for synthesizing chiral spirobilactams through double copper-catalyzed C–N couplings (Scheme 21).[63] Using diamides **73** as substrates and CuI/**L14** as a catalyst, the enantioselective tandem *N*-arylation proceeded smoothly. After filtering out the precipitate formed from the

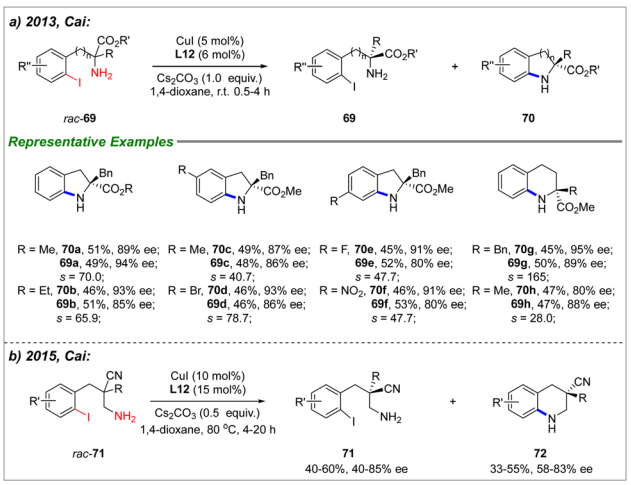

Scheme 20 Enantioselective C–N coupling *via* kinetic resolution process.

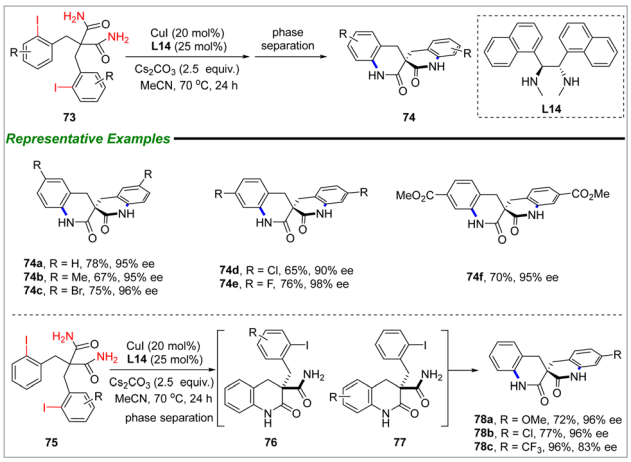

Scheme 21 Chiral spirobilactam synthesis *via* double *N*-arylation.

mixture, excellent enantioselectivities were achieved. The phase separation indicated an amplification of the products in solution, making this protocol a practical method for constructing a chiral spiro-based scaffold. When unsymmetrical substrates **75** were used, a mixture of **76** and **77** was obtained through the first *N*-arylation. The subsequent second C–N coupling then led to the synthesis of chiral spirobilactams **78** with excellent yields and enantioselectivities. Control experiments confirmed that the first C–N coupling was the stereo-determining step.

Following a similar approach, Sasai conducted a double *N*-arylation of diamine **79** for the enantioselective synthesis of a spiro framework (Scheme 22).[64] With the aid of chiral ligand **L15**, the spiro product **80** was obtained with 31% ee, which could be further increased to 99% through simple recrystallization. The subsequent removal of the Ts-group and installation of diphenylphosphine led to the synthesis of **82**, which could be used as a phosphine ligand. Combining **82** with stoichiometric palladium yielded the organopalladium complex **83**, which has potential applications in enantioselective catalysis.

In 2015, Cai reported the enantioselective synthesis of quinolinones **85** through a copper-mediated C–N coupling (Scheme 23a).[65] With the assistance of CuI/**L15**, the differences between two amides could be determined, allowing for the enantioselective C–N amination to proceed with moderate to good enantioselectivities. This protocol provided a new

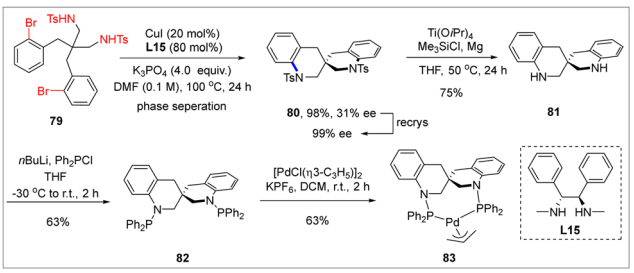

Scheme 22 Double *N*-arylation for enantioselective synthesis of diphenylphosphine.

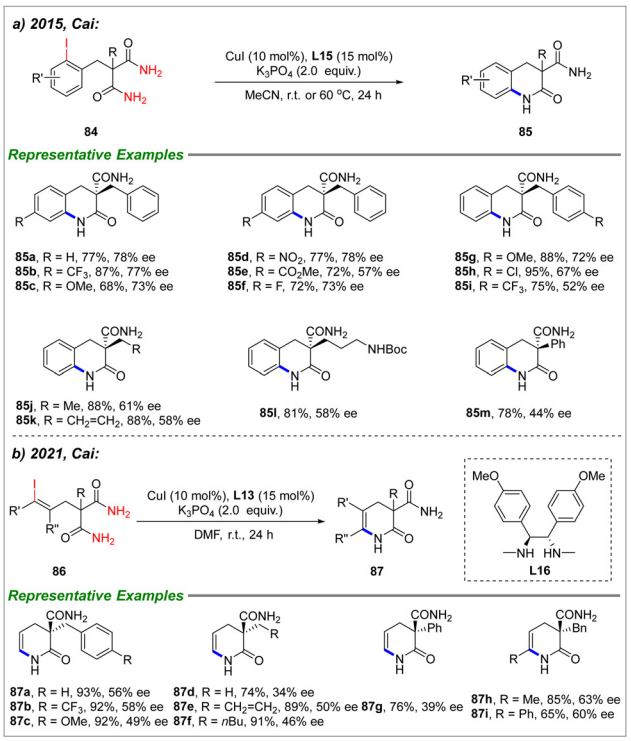

Scheme 23 Enantioselective C–N coupling *via* desymmetrization strategy.

pathway to chiral quinolinones bearing a quaternary stereocenter. More recently, vinyl iodides **86** were utilized in the enantioselective C–N amination using a desymmetrization strategy to afford 2-oxo-1,2,3,4-tetrahydro-pyridine-3-carboxamides **87** (Scheme 23b).[66] The enantioselective cyclization proceeded efficiently, although with relatively lower enantioselectivities. This methodology provides a readily accessible approach to constructing chiral heterocycles.

In 2019, Gu reported the intramolecular C–N amination for the synthesis of C–N atropisomers (Scheme 24).[67] Under the catalysis of CuTC/**L17**, a series of diverse functional C–N atropisomers were obtained with excellent yields and

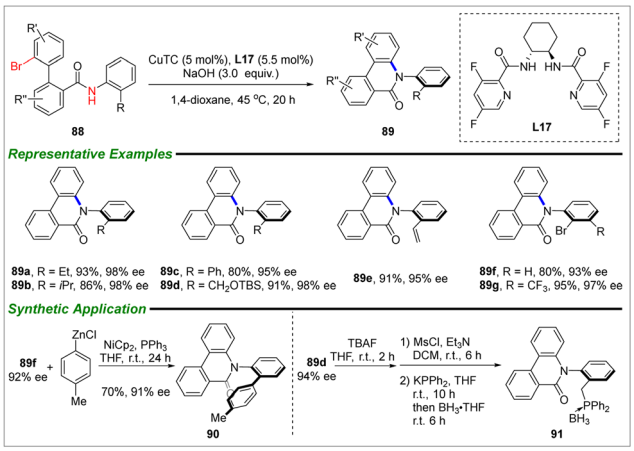

Scheme 24 Enantioselective intramolecular C–N coupling for C–N atropisomer synthesis.

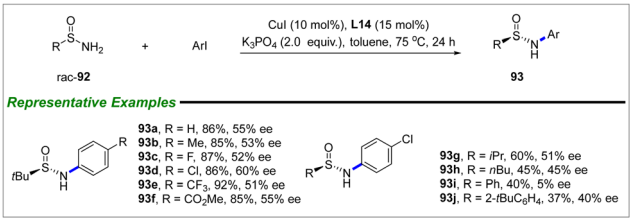

Scheme 25 Intramolecular C–N coupling *via* kinetic resolution strategy.

enantioselectivities. Notably, bromine-containing substrates were compatible with the protocol, delivering **89f** and **89g** with up to 97% ee. The utility of the enantioselective C–N coupling was demonstrated through the diverse transformation of the obtained C–N atropisomers. A cross-coupling of **89f** and an aryl zinc reagent proceeded smoothly with almost no loss of the ee value. Following a simple three-step route involving the removal of the TBS group, the formation of triflates, and the installation of phosphines, the C–N atropisomeric phosphine ligand **91** was obtained.

2.2.2 Intermolecular coupling. Besides intramolecular Ullmann-type C–N coupling, intermolecular type reaction is more appealing due to its divergent substrates scope. In 2016, Cai achieved intermolecular C–N coupling for chiral *N*-aryl sulfinamides through a kinetic resolution process (Scheme 25).[68] In the presence of CuI/**L14**, the C–N coupling of aryl iodides and sulfinamides was carried out successfully, resulting in moderate to excellent yields and moderate enantioselectivities.

In 2018, Miller reported the intramolecular enantioselective C–N coupling for the construction of central chirality, or both central and axial chirality (Scheme 26).[69] By using the threonine-based ligand **L18**, the copper-catalyzed C–N coupling proceeded smoothly to afford mono *N*-arylation products **95**

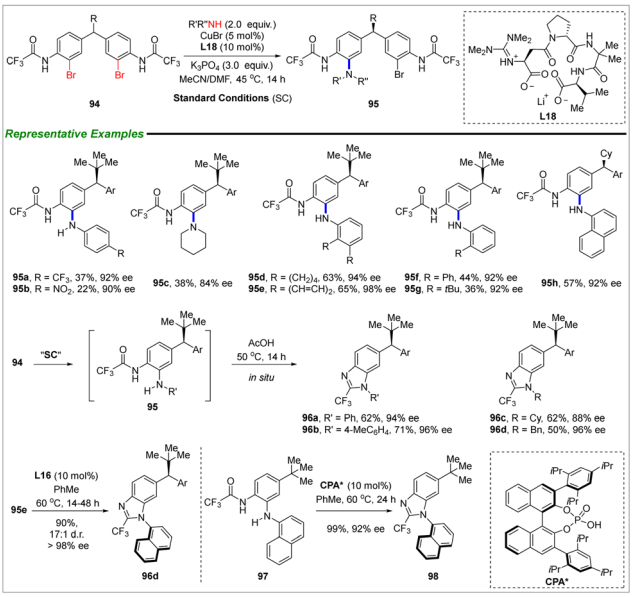

Scheme 26 Enantioselective C–N coupling for the construction of central and axial chirality.

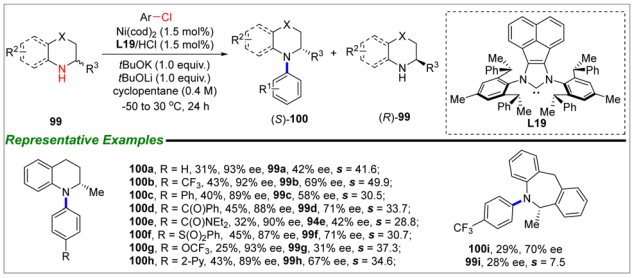

Scheme 27 Nickel/NHC-catalyzed enantioselective C–N cross coupling.

with excellent enantioselectivities. The obtained **95** underwent cyclodehydration to form the heterocycle **96** *in situ* with AcOH. Additionally, the *N*-arylated **95e** underwent cyclization to produce **96d** diastereoselectively under the catalysis of chiral phosphoric acid **CPA***. When achiral arylamine **97** was used as the substrate, enantioselective cyclization was achieved to yield **98** with 92% ee.

2.3 Nickel-catalyzed enantioselective C–N coupling

The utility of non-noble metal such as nickel could improve the applicability of C–N coupling greatly. In 2021, Shi and Hong successfully achieved the nickel-catalyzed enantioselective C–N coupling of aryl chlorides and tetrahydroquinolines using a kinetic resolution strategy (Scheme 27).[70] The reaction took place under low-temperature conditions, reaching as low as −50 °C, which demonstrated the high reactivity of the nickel/N-heterocyclic carbene (NHC) catalyst. DFT calculations showed that the catalyst system was responsible for the oxidative addition, reductive elimination, and stereocontrol processes. With the aid of nickel/**L19**, a series of chiral arylated amines with diverse functional groups could be obtained, along with unreacted amines, all with excellent enantioselectivities.

2.4 Enantioselective Chan–Evans–Lam coupling

Cu-catalyzed Chan–Evans–Lam C–N coupling is a highly efficient approach for constructing C–N bonds, but achieving asymmetric synthesis remains challenging.[71–74] Recently, Patureau and Ikawa independently developed the enantioselective Chan–Evans–Lam coupling for synthesizing C–N atropisomers.[75,76]

Patureau reported the enantioselective C–N coupling of benzimidazoles **101** with *ortho*-substituted aryl boronic acid for the synthesis of C–N atropisomers (Scheme 28a).[75] With the aid of N,N-chelated ligand **L20**, the enantioselective Chan–Evans–Lam coupling proceeded readily to afford the desired products **102** with up to 92% ee. To gain insight into the stereocontrol process, a possible mechanism was proposed. Initially, Cu^{I} coordinated with **L20** under oxidative conditions to deliver **INT-6** Cu^{II}, which then reacted with benzimidazoles and arylboronic acid to form **INT-7**. Subsequently, **INT-7** was oxidized to Cu^{III} complex **INT-8**, leading to the formation of the final product **102** through reductive elimination. The resulting Cu^{I} complex **INT-9** could be oxidized to Cu^{II} complex **INT-5** to complete the catalytic cycle.

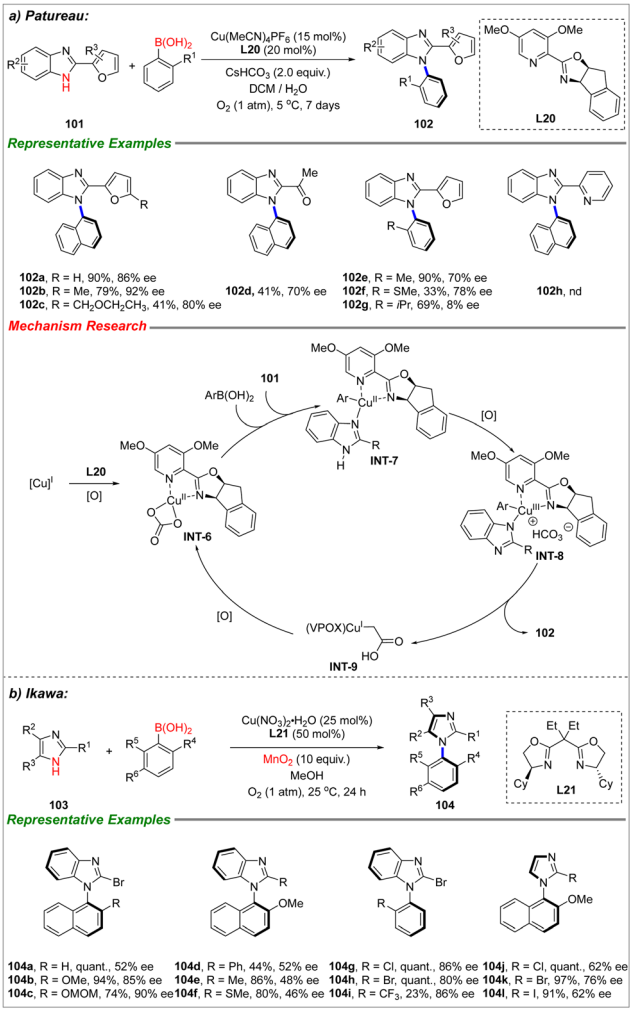

Scheme 28 Enantioselective Chan–Evans–Lam coupling.

At the same time, Ikawa reported a similar C–N coupling of imidazoles and arylboronic acid for the synthesis of C–N atropisomers (Scheme 28b).[76] With the catalysis of copper/**L21**, a series of divergent functional C–N atropisomers **104** could be achieved with moderate to excellent enantioselectivities. Control experiments demonstrated that the addition of MnO_2 was crucial for the success of the enantioselective synthesis.

3. Diaryliodonium salt-mediated C(sp^2)–N cross-coupling

Diaryliodonium salts, a type of hypervalent iodine(III) compound, have been extensively studied for over the last century due to their easy availability, air and moisture stability, and high reactivity.[77,78] In the past decade, cyclic diaryliodonium salts have been used to facilitate ring-opening reactions to yield coupling products featuring a remaining iodine group.[13]

With the recent increase in interest in synthesizing C–N/N–N atropisomers, a range of diaryliodonium salt-mediated C(sp^2)–N cross-couplings have been developed. The copper-mediated

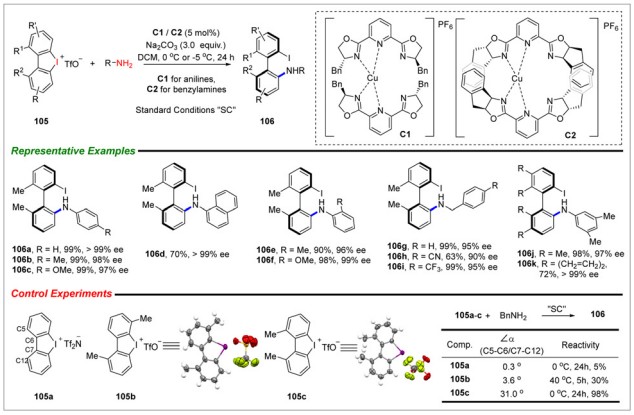

Scheme 29 Enantioselective ring-opening reaction of cyclic aryliodonium.

enantioselective C(sp^2)–N cross-coupling with amines as nucleophiles has been proven to be a highly efficient system, delivering centered chiral compounds as well as C–C/C–N atropisomers. Additionally, the iodine group of the coupling products can be easily converted into diverse functional groups, which is crucial for expanding the potential applications of these couplings.

3.1 Cyclic aryliodonium-mediated C–C atropisomer synthesis

In 2018, Gu disclosed the copper-catalyzed ring-opening reaction of cyclic aryliodonium to afford C–C atropisomers (Scheme 29).[79] With copper/bis(oxazolinyl)pyridine complex **C1** or **C2** as catalysts, the C–N coupling was conducted under mild conditions, resulting in axially chiral products **106** with excellent yields and enantioselectivities. To gain insight into the mechanism, a series of control experiments were carried out. The structures of substrates with none, one, or two substituents were compared using X-ray diffraction of single crystal structures, revealing increasing dihedral angles ranging from 0.3° to 31.0°. This study suggested that **105c** exhibited significantly higher distorted energy and reaction reactivity, consistent with the observed results in the ring-opening reaction.

Gu successfully extended the substrate scope of enantioselective ring-opening synthesis to benzylic or aliphatic amines (Scheme 30).[80] The key procedure ensuring excellent enantio-

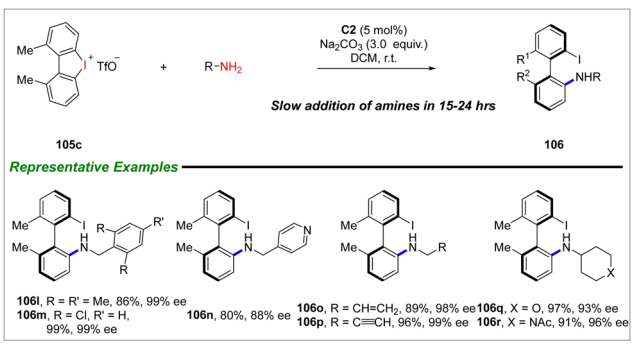

Scheme 30 Enantioselective ring-opening reaction with aliphatic amines.

selectivity involved maintaining low concentrations of the amines through their slow addition. Higher concentrations of amines can destabilize the chiral catalyst due to the competitive coordination of copper, resulting in lower efficiency of stereoinduction. The protocol demonstrated a broad substrate scope, high efficiency, and excellent enantioselectivities.

The aforementioned atropisomer synthesis is not applicable to sterically hindered amines; therefore, a more efficient catalyst system needs to be developed to address this challenge. In 2020, Gu reported the chiral anionic cobalt(III)-assisted ring-opening reaction for the synthesis of axially chiral biaryl amines (Scheme 31).[81] With a catalytic amount of chiral anionic catalyst, the ligand-free copper was able to facilitate the enantioselective synthesis smoothly, achieving excellent enantioselectivities. It should be noted that the coupling counterparts could be comparable with bulky amines, including *ortho*-disubstituted arylamines. To gain a better understanding of the mechanism, a cobalt-containing substrate **107** was synthesized through the anion exchange of cyclic aryliodonium with stoichiometric **A1**. Then, **107** was utilized as a catalyst in the ring-opening reaction, resulting in the formation of **106s** with 95% ee. Control experiments suggested that the *in situ* formed substrate–anion complex was probably the catalyst.

With the cyclic aryliodonium **105** as the reaction counterpart, a series of N-nucleophiles were applied to the ring-opening reaction (Scheme 32(a)).[82] *O*-alkylhydroxylamines **108** behaved as suitable coupling partners in the copper-mediated enantioselective ring-opening reaction. The choice of CaO as the base was a key element of the protocol, significantly increasing the enantioselectivities and reducing the formation of side products. This led to the successful synthesis of diverse functional 2-hydroxyamino-2′-iodobiaryls **109** with excellent yields and enantioselectivities.

1,2,3-Triazoles were also utilized in enantioselective ring-opening reactions with the catalytic system $Cu(MeCN)_4PF_6$/(*S*,*S*)-PhBOX (Scheme 32b).[83] This catalytic system exhibited excellent chemo-selectivity in distinguishing between the three nitrogen atoms present in 1,2,3-triazoles. The resulting products **111c** with 96% ee could be readily transformed to chiral phosphine ligand **112** with minimal loss of enantioselectivity, highlighting the effectiveness and utility of this protocol.

Oximes can also be used as substrates to afford *N*-arylation in a ring-opening reaction with excellent chemo-selectivity (Scheme 32c).[84] Under the catalysis of $Cu(MeCN)_4PF_6$/(*S*,*S*)-PhBOX, the atropisomeric nitrones **114** were obtained with excellent enantioselectivities. The resulting nitrones **114a** could be readily converted to biaryls **115** bearing a heterocycle with 100% enantioselectivity.

Imides have also been proven to be good coupling partners in the ring-opening of diaryliodonium salts (Scheme 32d).[85] With the aid of **L22**, a series of axially chiral 2-imidobiaryls were afforded with excellent yields and enantioselectivities. This chemistry provided a new route to obtain the N,P-ligand **118a** or N,N-ligand **118b** with 99% ee, showcasing its potential for applications in enantioselective synthesis.

In addition to these achievements, the three-component ring-opening reaction for biaryl atropisomers has also been reported.[86]

3.2 Diaryliodonium-mediated C–N atropisomer synthesis

In 2018, Colobert and Wencel-Delord developed an Ullmann-type *N*-arylation for the synthesis of C–N atropisomers (Scheme 33).[12] By using a chiral sulfoxide auxiliary, the copper-catalyzed C–N coupling was able to proceed smoothly under mild conditions, thus avoiding the need for high temperatures typically required in Ullmann-type reactions. The protocol successfully yielded C–N atropisomer **121** with good to excellent enantioselectivities. A possible mechanism was proposed to explain the stereocontrol process. The catalytic cycles began with the combination of indolines **120** with the *in situ* formed copper complex to deliver **INT-10**. Subsequent chelation of the sulfoxide group with **INT-10** afforded **INT-11**, which was then transformed to **INT-12**. The excellent enantioselectivity observed can be attributed to the π-interaction between the sulfoxide group and the indoline in **INT-12**, while **INT-12′** was found to be less favorable. The catalytic cycles were completed through reductive elimination, leading to the formation of the C–N atropisomers.

In 2020, Wencel-Delord reported the catalytic enantioselective synthesis of C–N atropisomers through Ullmann-type cross-coupling (Scheme 34).[87] The enantioselective *N*-arylation proceeded smoothly at room temperature using (*R*,*R*)-BnBOX as a ligand, delivering a series of C–N atropisomers with moderate to good yields and up to 98% ee. This protocol represents the first catalytic enantioselective synthesis of C–N atropisomers with hypervalent iodines, affording C–N atropisomeric scaffolds of pharmaceutical value.

3.3 Cyclic aryliodonium-mediated centered enantiomer synthesis

In 2020, Yang, Yu, and Jin reported the enantioselective ring-opening reaction of a six-member cyclic aryliodonium *via* copper-catalyzed cross-coupling (Scheme 35).[88] The methodology featured less nucleophilic sulfonamides **126** as substrates, affording aryl iodides bearing central chirality. A variety of ring-opening products

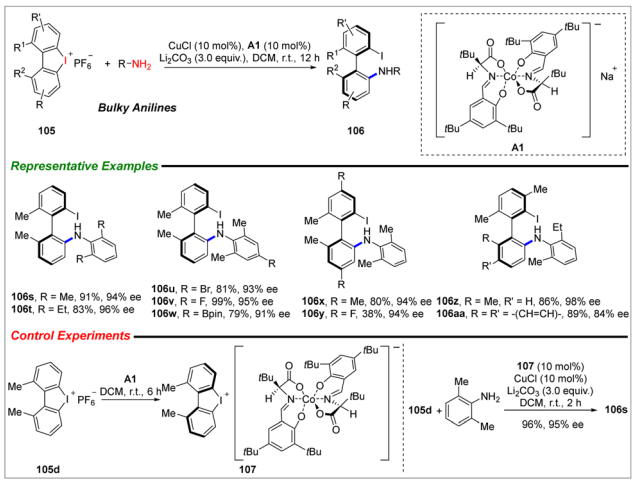

Scheme 31 Chiral anion-assisted enantioselective ring-opening of cyclic aryliodonium.

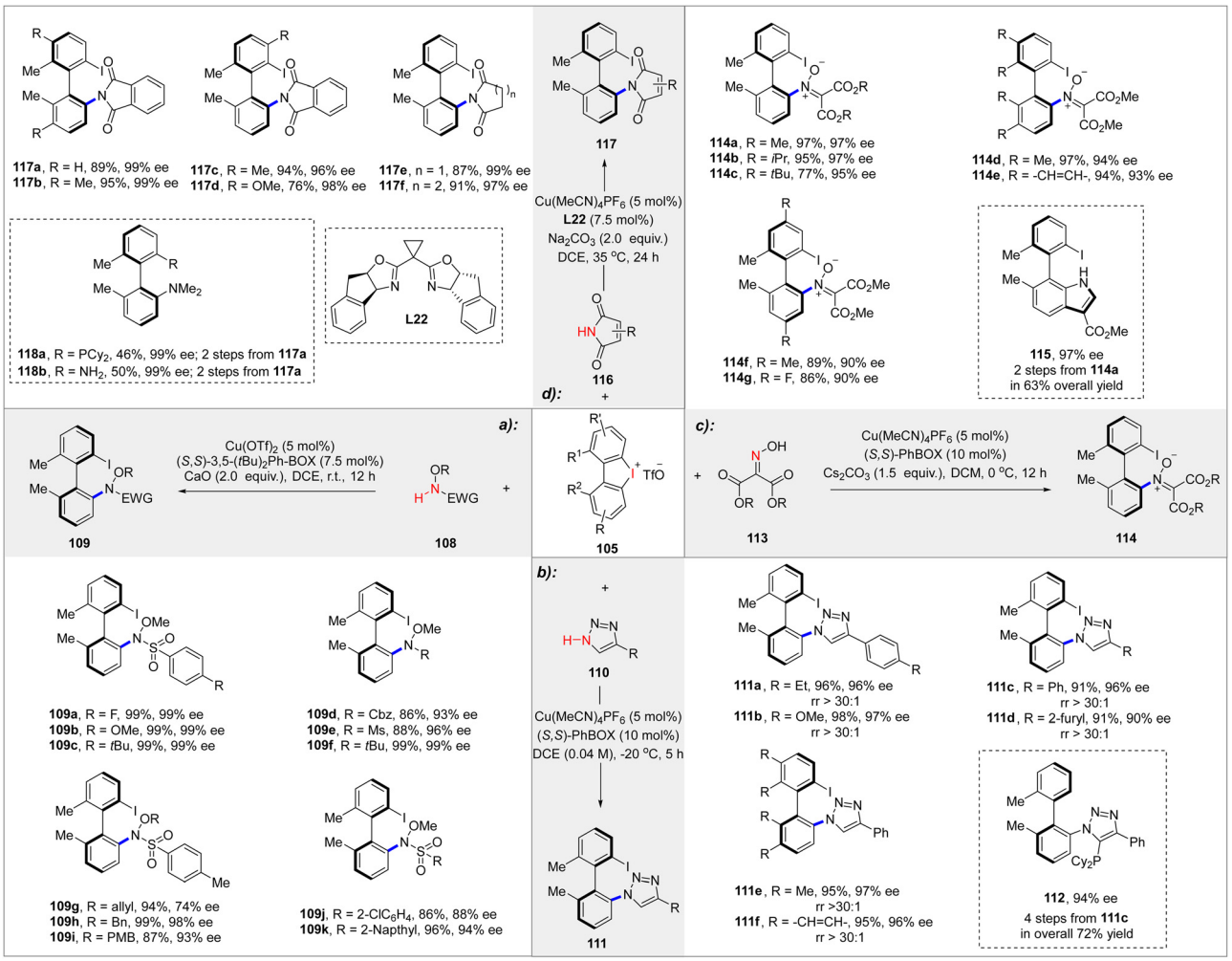

Scheme 32 Enantioselective ring-opening of cyclic aryliodonium with other *N*-nucleophiles.

with diverse functional groups were obtained with good to excellent enantioselectivities.

4. Enantioselective C(sp^3)–N cross-coupling involving radicals

The radical is a robust intermediate with high reactivity, commonly used in organic transformations. Harnessing highly reactive radicals and applying them to enantioselective synthesis has been a long-standing challenge in recent decades.[89–92] Following Fu's pioneering work on photoinduced enantioselective copper-catalyzed C–N cross-couplings in 2016, there has been a resurgence in radical-involved C–N coupling chemistry.[16] This chemistry combines earth-abundant transition metal copper and radical precursors to smoothly afford chiral alkyl amines, greatly expanding the scope and practicality of C–N couplings.

4.1 Photoinduced enantioselective C(sp^3)–N cross-coupling

In 2016, Fu achieved copper-catalyzed C–N coupling using blue light irradiation for tertiary alkyl amines bearing central chirality (Scheme 36).[16] By using the monophosphine **L23**, the enantioselective coupling proceeded efficiently, yielding **130** with excellent enantioselectivities. A crystal of the complex of copper, substrate **129a**, and **L23** was grown and analyzed through X-ray diffraction, providing insight into the enantioselective catalytic process. When complex **131** was used as a substrate to react with **128a** under blue light, the desired product **130g** was obtained in a 72% yield with 92% ee, while no reaction occurred without light. These results suggest that **131** may be the catalyst in the C–N coupling process. Additionally, when enantioenriched substrate **128a** was used, both (+)-**128a** and (−)-**128a** converted to (*R*)-**130g** under standard conditions, eliminating the possibility of kinetic resolution. Based on mechanistic studies, a probable mechanism was proposed involving the *in situ* formation of copper complex **INT-14** reacting with carbazoles to form **INT-15**, which then undergoes oxidative addition with alkyl bromides to yield **INT-16**. A possible radical-involved intermediate **INT-16** or a copper-nucleophile complex **INT-16′** eventually transforms to the final product through reductive elimination, completing the catalytic cycle.

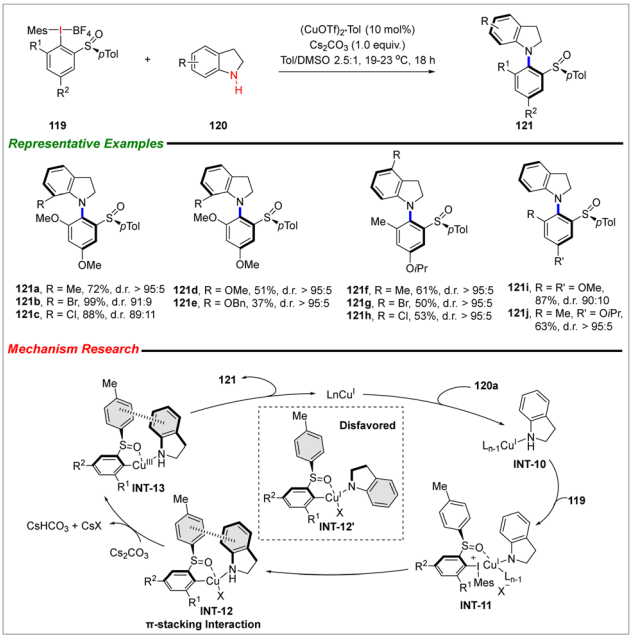

Scheme 33 Copper-catalyzed C–N coupling for C–N atropisomer synthesis.

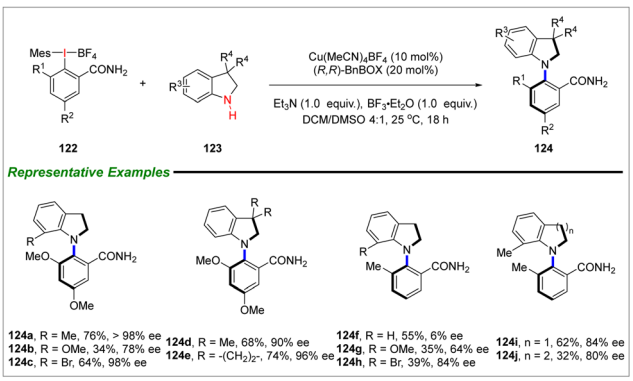

Scheme 34 Catalytic enantioselective C–N coupling for C–N atropisomers.

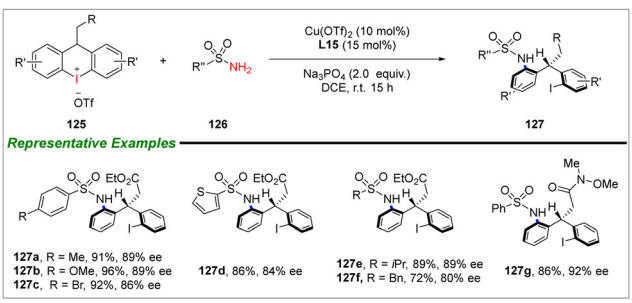

Scheme 35 Enantioselective C–N coupling reaction for central chirality construction.

Recently, Peters and Fu conducted a detailed investigation into the mechanism of light-induced enantioselective C–N

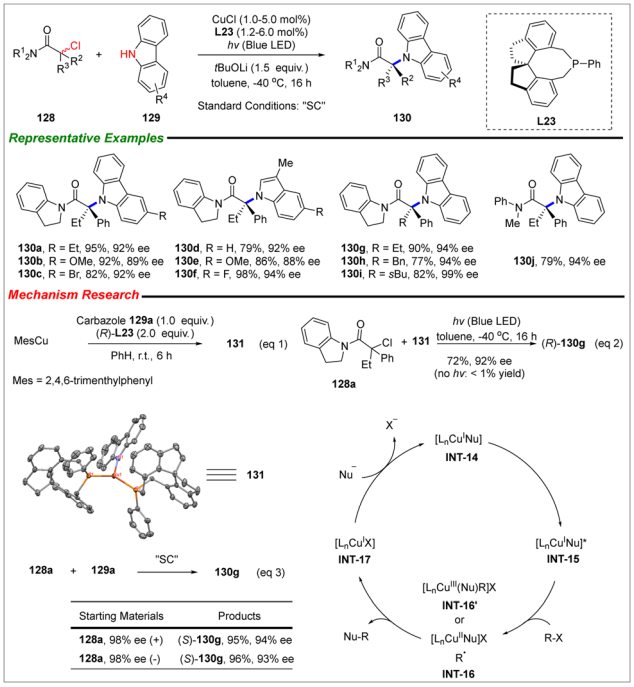

Scheme 36 Blue light-assisted enantioselective C–N coupling.

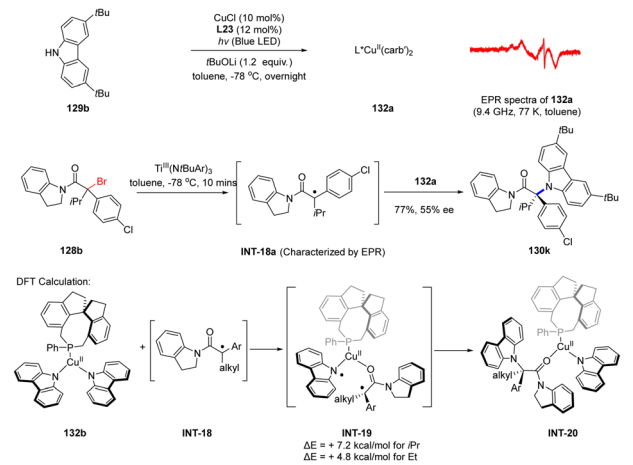

Scheme 37 Mechanistic studies on light-induced enantioselective C–N coupling.

coupling (Scheme 37).[93] First, they synthesized and characterized the complex of **128a** and carbazoles **129b** using EPR, which exhibited a clear signal. Subsequently, **128b** reacted with [Ti^{III}] to form a radical intermediate that was confirmed by EPR. Treatment with **132a** then led to the formation of the C–N coupling product **130K** with 55% ee. According to DFT calculations, **132b** would coordinate with the radical intermediate **INT-18** through the carbonyl oxygen (ΔE = 4.8–7.1 kcal mol^{-1}), resulting in the formation of **INT-19**, which serves as the precursor to **INT-20**. Mechanistic studies revealed a radical-involved process for light-induced enantioselective C–N coupling.

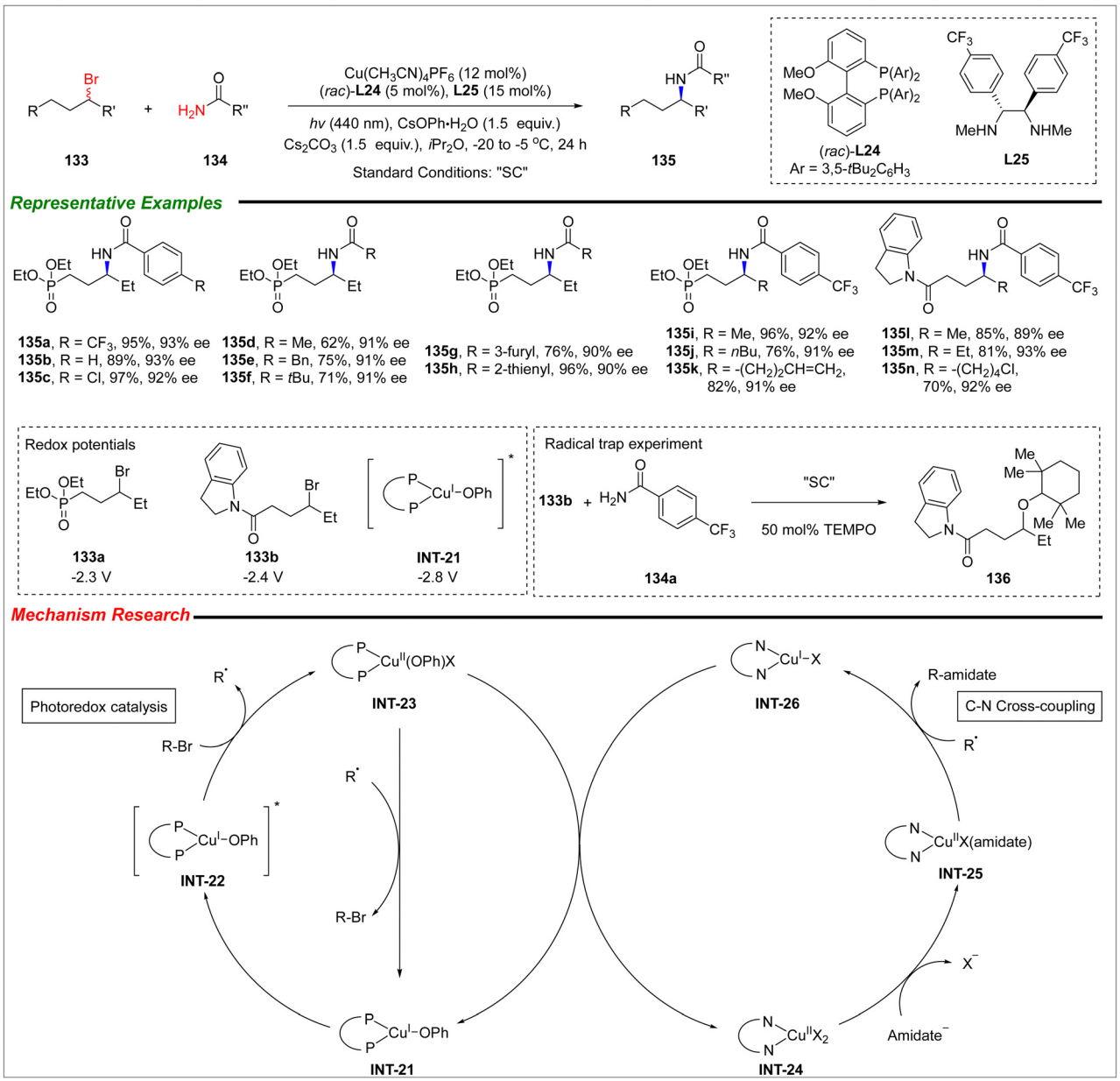

Scheme 38 Photoinduced enantioselective C–N coupling with amides as nucleophiles.

In 2021, Fu reported the photoinduced enantioselective C–N cross-coupling with amides as nucleophiles (Scheme 38).[94] The copper-mediated catalysis system featured a copper–biphosphine catalyst for the activation of alkyl bromides and a copper–diamine catalyst for enantioselective C–N coupling. The enantioselective *N*-arylation stimulated by blue light proceeded smoothly, yielding a series of functional chiral amides with excellent enantioselectivities. The redox potentials of alkyl bromides **133a**, **133b**, and copper–biphosphines **INT-21** were calculated, indicating that the lower potentials of **INT-21** could activate the substrates **133** under photocatalysis. The radical-trap experiment under standard conditions only afforded the radical-terminated product **136**, indicating a possible radical-involved process. Following mechanistic studies, a possible mechanism involving both photoredox catalysis and C–N cross-coupling catalysis was proposed. Irradiation with blue light enabled **INT-21** to produce **INT-22**, which could activate alkyl bromides to form alkyl radicals. The oxidation of **INT-26** with **INT-23** delivered **INT-24**, which then led to the formation of **INT-25** by the substitution of X with the amide anion. The radical subsequently reacted with **INT-25** to form the final C–N coupling product.

The photoinduced enantioselective C–N coupling strategy could be further extended to the construction of quaternary stereocenters. In 2022, Fu and Peters reported the enantioselective C–N cross-coupling for the synthesis of chiral amines bearing a chiral quaternary carbon center (Scheme 39).[95] Under the catalysis of CuCl/(*R*)-DTBM-SEGPHOS, a series of diverse

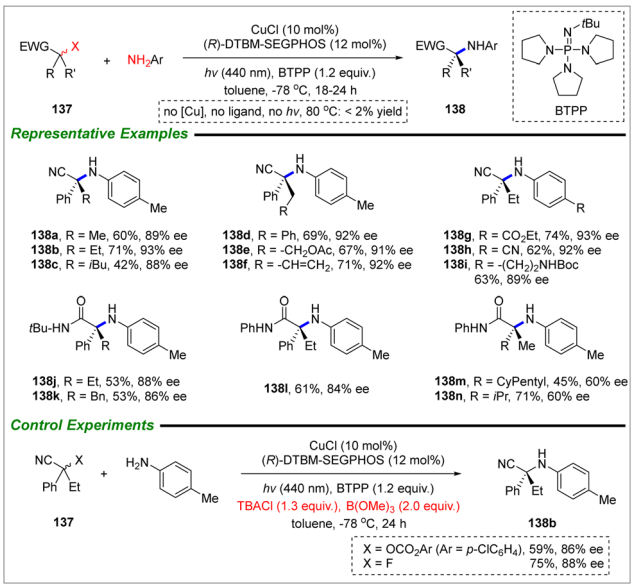

Scheme 39 Enantioselective C–N coupling of alkyl chlorides and arylamines.

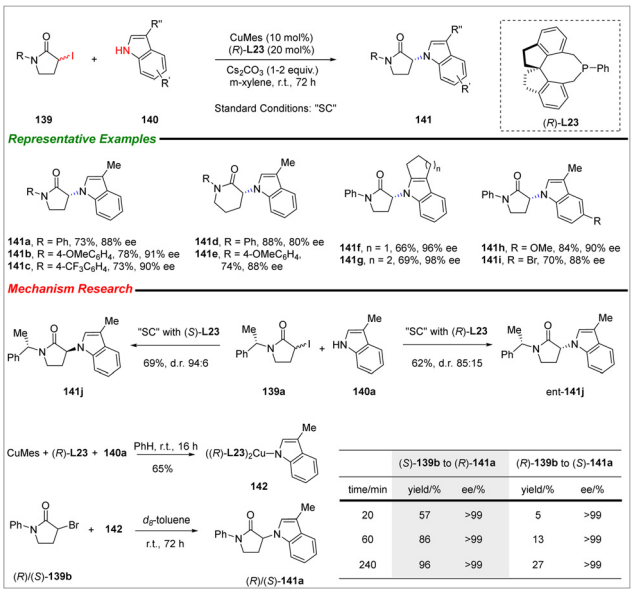

Scheme 40 Enantioselective nucleophilic substitution for central chirality construction.

functional chiral alkyl amines could be obtained at −78 °C with excellent enantioselectivities. In the absence of copper, ligand, and blue light, almost no reaction of **137** with arylamine was observed, even at 80 °C, indicating the high efficiency of the catalytic system in terms of reactivity and enantioselectivity for the coupling reaction. Addition of TBACl/$B(OMe)_3$ allowed for the use of carbonates or fluorides as excellent chloride surrogates in the enantioselective C–N coupling. This represents the first example of fluorides serving as electrophiles in a transition-metal-mediated *N*-arylation reaction.

4.2 Other radical-mediated enantioselective C(sp^3)–N cross-couplings

In 2019, Fu reported the enantioselective copper-catalyzed C–N coupling in the absence of light (Scheme 40).[96] The reaction involved the copper-mediated nucleophilic substitution of racemic alkyl iodides **139** with indoles **140** to afford chiral amines **141**. This approach addressed the limitations of the classic S_N2 type reaction, which typically exhibited low reactivity and lacked stereoinduction. A series of amines bearing a tertiary stereocenter were obtained with excellent enantioselectivities. Notably, when using **139a** with a defined stereocenter, the configuration of the newly formed stereocenter was solely determined by the chirality of the ligand. A copper complex was prepared from CuMes, (*R*)-**L23**, and indoles **140a**, which was then employed in the enantioselective C–N coupling with (*R*)/(*S*)-**139b**. It was observed that the reaction rate of (*S*)-**139b** was ten times that of (*R*)-**139b**, suggesting a significant match/mismatch relationship between the chirality of the alkyl bromide and the ligand.

In 2021, Liu achieved the enantioselective *N*-arylation of sulfoximines *via* a copper-catalyzed C–N cross-coupling (Scheme 41).[97] With the catalysis of copper and a novel N,N,P-chelated ligand, a wide range of chiral sulfoximines

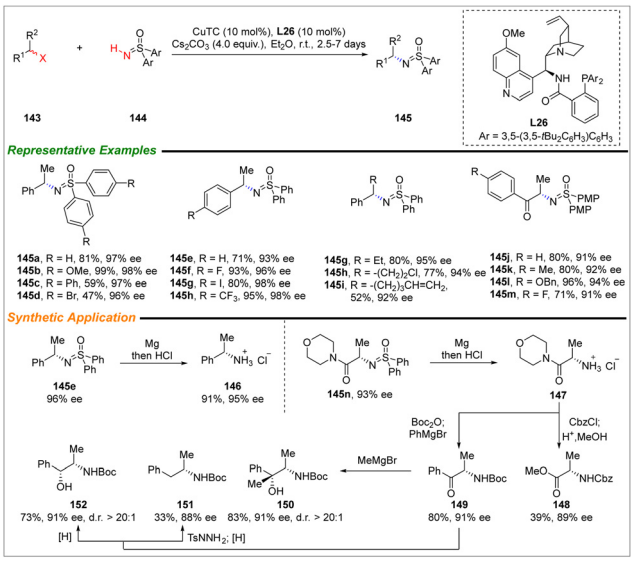

Scheme 41 Enantioselective C–N coupling for chiral masked primary amines.

145 were obtained with excellent enantioselectivities. The masked primary amines **145** could then be converted into a series of useful building blocks. Treatment of **145e** (96% ee) with magnesium, followed by acidification, yielded a chiral ammonium salt in 91% yield and 95% ee. In the case of **145n**, the resulting ammonium salt **147** could be transformed into α-N-substituted ester **148** with 89% ee. Phenyl-substituted **149** reacted with MeMgBr or was directly reduced to produce α-amino alcohol **152** with excellent diastereoselectivities (d.r. > 20 : 1). Reaction with $TsNHNH_2$ and subsequent reduction led to the conversion of **149** to alkyl amine **152** with 88% ee, albeit

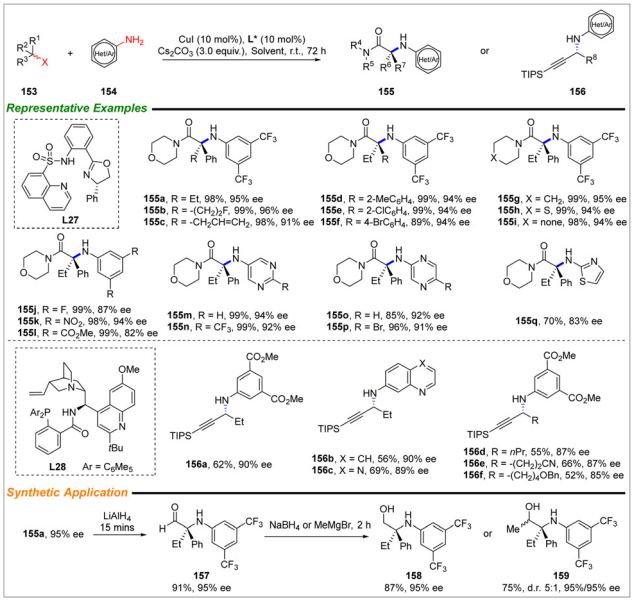

Scheme 42 Enantioselective C–N coupling of diverse functional alkyl halides.

in a yield of 33%. These diverse transformations highlighted the utility of this protocol.

In 2023, Liu reported the copper-catalyzed enantioselective C–N coupling of alkyl halides and (hetero)aryl amines using a radical-involved process under ambient conditions (Scheme 42).[98] The key to the success of this reaction was the selectivity of the appropriate ligand with different alkyl halides. When using the N,N,N-chelated ligand **L27**, α-chloro-amides served as suitable reaction counterparts in the enantioselective *N*-arylation. In the case of alkynyl chlorides, the quinine-based ligand **L28** proved to be efficient in promoting the enantioselective C–N coupling. With the appropriate ligands, the protocol proceeded smoothly, yielding a variety of functional chiral amines with excellent enantioselectivities. The newly formed enantioenriched **155a** could be readily converted to α-amino aldehydes **157**, which could then be further transformed into α-amino alcohols **158** or **159** with 100% enantioselectivity upon subsequent reduction or methyl addition.

In 2023, Liu achieved the enantioselective C–N coupling of α-bromo-β-lactam **160** through a copper-mediated radical-involved process (Scheme 43).[99] Under the catalysis of CuI/oxazoline-derived ligand **L29**, the chiral α-amino-β-lactams **161** were obtained with excellent enantioselectivities. However, when TEMPO was added under standard conditions, no reaction occurred. By adding the radical scavenging reagent BHT, the radical-trapped product **162** was obtained in a yield of 57%. The mechanistic studies conducted suggested that the protocol may proceed through a radical-involved process.

Recently, Liu reported a copper-mediated radical-involved C–N cross-coupling for synthesizing chiral bulky amines (Scheme 44).[100] By using the N,N,N-chelating ligand **L30**, the enantioselective *N*-arylation proceeded smoothly, resulting in the formation of chiral amines **165** with excellent enantioselectivities. A possible mechanism was proposed, which suggested

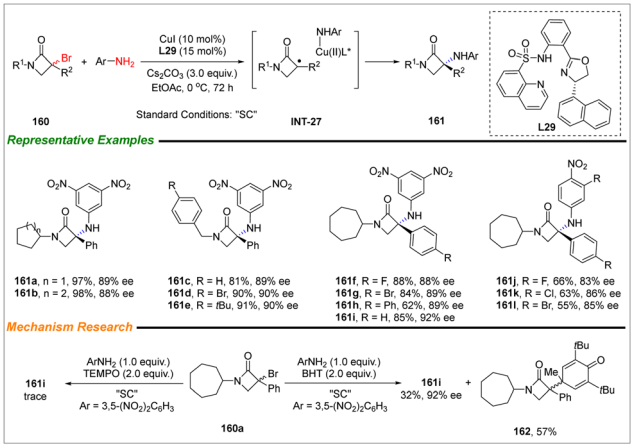

Scheme 43 Enantioselective C–N coupling for chiral α-amino-β-lactam synthesis.

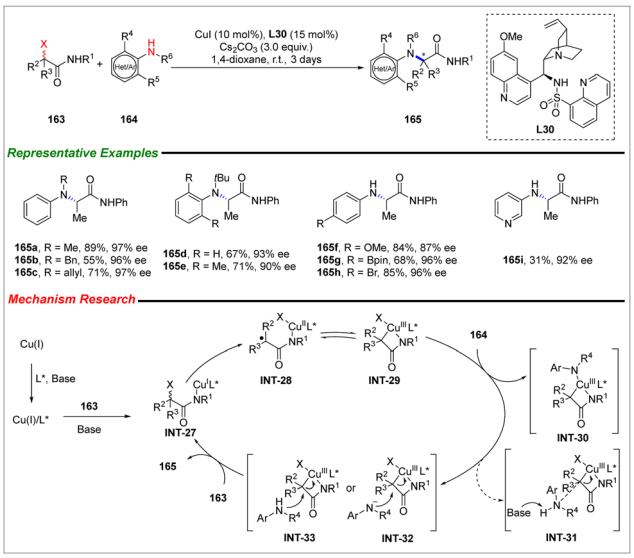

Scheme 44 Enantioselective C–N coupling for chiral bulky amine synthesis.

an out-sphere *N*-substitution process. The *in situ* formed CuI reacted with **163** to yield **INT-27**, which then underwent conversion to **INT-29** and **INT-30** in equilibrium. Subsequent out-sphere *N*-substitution *via* **INT-32** or **INT-33** led to the formation of the final products **165**. The inner-sphere process involving reductive elimination through **INT-30** was unlikely. The outer-sphere N-attack model explained the excellent reactivity of bulky amines in enantioselective synthesis.

Aliphatic amines are highly reactive, but their application in copper-mediated enantioselective synthesis is limited due to transition-metal-catalyst poisoning and challenges in stereocontrol. In 2023, Liu successfully utilized these reactive aliphatic amines in enantioselective C–N coupling with the N,N,N-chelating ligand **L30** (Scheme 45).[101] This approach enabled the enantioselective *N*-alkylation of aliphatic amines **166** with alkyl chlorides **163** to proceed smoothly, resulting in the formation of chiral amines **167** with excellent enantioselectivities. The

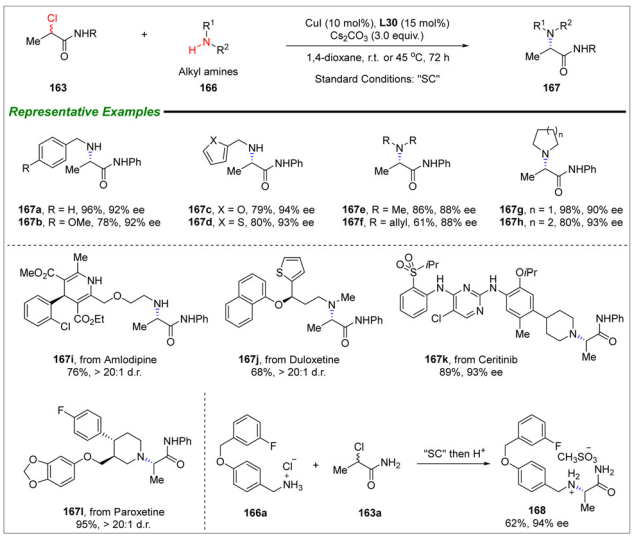

Scheme 45 Copper-catalyzed enantioselective *N*-alkylation of aliphatic amines.

wide substrate scope of this method was demonstrated by its successful application in the synthesis of bioactive and drug-like molecules. Additionally, the compatibility of the protocol with the use of ammonium salt **166a** led to the formation of **168** with 94% ee. The use of the multi-chelated ligand **L30** was crucial in overcoming the issue of catalyst poisoning by aliphatic amines, ultimately leading to excellent enantioselectivities.

In 2023, Fu estimated the copper-mediated enantioselective C–N coupling of α-chloroboronate ester **169** and carbamate **170** to afford α-aminoboronic derivatives **171** (Scheme 46).[102] Control experiments indicated that copper complex **172** would convert to biarylphosphane **173** under the irritation of blue light. The combination of CuCl, diamine ligand **L15**, and **173** could catalyze the enantioselective C–N coupling to give the desired product **171b** in a 36% yield with 77% ee. Therefore, biarylphosphane **L32** was utilized to co-catalyze the enantioselective synthesis after screening reaction conditions. With the

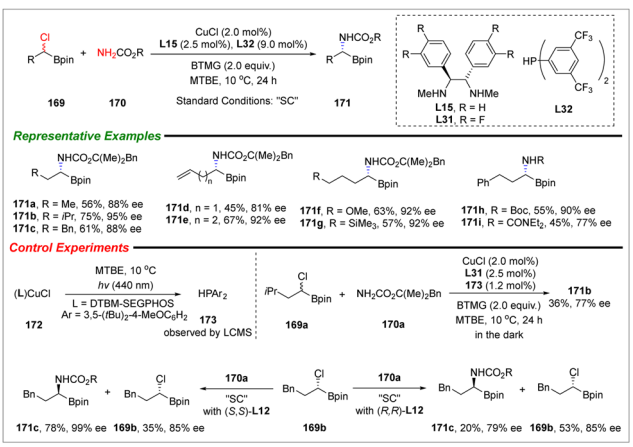

Scheme 46 Copper-catalyzed enantioselective C–N coupling for α-aminoboronic derivative synthesis.

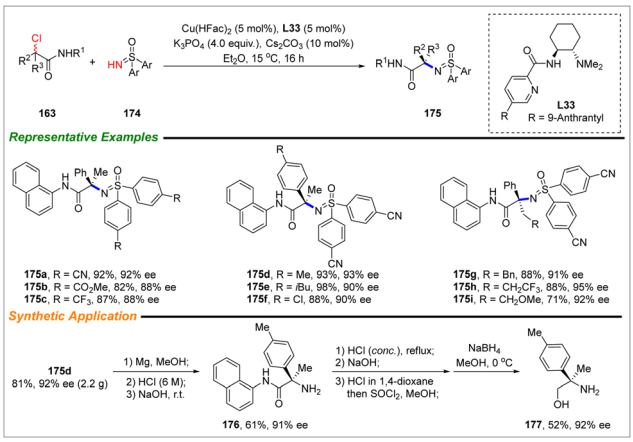

Scheme 47 Enantioselective C–N cross coupling for chiral sulfoximine synthesis.

catalysis of CuCl, **L14**, and **L32**, a series of divergent functional α-aminoboronic derivatives could be achieved with good to excellent enantioselectivities. When enantiomer **169b** was used, the catalyst system bearing (*S,S*)-**L15** or (*R,R*)-**L15** showed a different reaction rate, indicating a kinetic resolution process.

In 2023, Liu reported on the copper-catalyzed enantioselective C–N coupling for the synthesis of chiral sulfoximines (Scheme 47).[103] The use of the N,N,N-chelated ligand **L33** with a long side arm played a crucial role in the success of this reaction. The enantioselective *N*-alkylation of **174** with **163** as nucleophiles proceeded under mild conditions, resulting in the formation of chiral sulfoximines **175** with excellent enantioselectivities. The newly formed amines could be readily converted to chiral amine building blocks, such as chiral amino alcohol **177** bearing a quaternary chiral carbon center, in just a few steps.

5. Conclusions and perspectives

Based on enantioselective C–N cross-coupling, palladium-catalyzed enantioselective C–N coupling (enantioselective Buchwald–Hartwig reaction), copper-catalyzed enantioselective C–N coupling (enantioselective Ullmann reaction), copper-catalyzed enantioselective ring-opening reaction of cyclic aryliodonium, and copper-catalyzed enantioselective radical C–N coupling have been extensively developed. Despite the significant progress achieved, there is a strong need to explore new reactions and strategies due to their vital importance in both academia and industry.

The focus of transition metals in enantioselective C–N couplings has primarily centered on palladium and copper. It is essential to diversify the use of transition metals, with a particular emphasis on non-noble metals such as nickel or iron, known for their excellent coupling abilities, to further expand the industrial applications of these reactions.

The design of ligands plays a crucial role in enantioselective C–N coupling, as demonstrated by the evaluation of ligands in the Buchwald–Hartwig and Ullmann reactions. The development of

novel ligands has significantly broadened the scope and generality of the enantioselective Buchwald–Hartwig reaction. In the case of enantioselective radical C–N coupling of aliphatic amines, the use of multi-chelated ligands is pivotal. Therefore, structurally diverse ligands must be developed and applied to advance enantioselective C–N couplings.

Author contributions

R. R. L. proposed the topic of the review. J. F., L. X., C. L., and R.R. L. investigated the literature. J. F. wrote the original draft of the manuscript. R. R. L. revised the manuscript.

Data availability

Data sharing is not applicable to this article as no datasets were generated or analysed during the current study.

Conflicts of interest

The authors declare no competing interests

Acknowledgements

Financial support from the Taishan Scholar Youth Expert Program in Shandong Province (tsqn 201909096, tsqn 202312165), National Natural Science Foundation of China (22371152, 22271169), and National Natural Science Foundation of Shandong (ZR2023JQ006, ZR2022MB021) is gratefully acknowledged.

Notes and references

1 T. C. Nugent, *Chiral Amine Synthesis: Methods, Developments, and Applications*, Wiley-VCH, Weinheim, 2010, pp. 1–459.
2 F. Ullmann, *Ber. Dtsch. Chem. Ges.*, 1903, **36**, 2382–2384.
3 A. S. Guram, R. A. Rennels and S. L. Buchwald, *Angew. Chem., Int. Ed. Engl.*, 1995, **34**, 1348–1350.
4 J. Louie and J. F. Hartwig, *Tetrahedron Lett.*, 1995, **36**, 3609–3612.
5 M. Breuer, K. Ditrich, T. Habicher, B. Hauer, M. Keßeler, R. Stürmer and T. Zelinski, *Angew. Chem., Int. Ed.*, 2004, **43**, 788–824.
6 O. I. Afanasyev, E. Kuchuk, D. L. Usanov and D. Chusov, *Chem. Rev.*, 2019, **119**, 11857–11911.
7 F. Zhou and Q. Cai, *Beilstein J. Org. Chem.*, 2015, **11**, 2600–2615.
8 J. F. Hartwig, *Acc. Chem. Res.*, 2008, **41**, 1534–1544.
9 V. V. Zhdankin and P. J. Stang, *Chem. Rev.*, 2008, **108**, 5299–5358.
10 A. Yoshimura and V. V. Zhdankin, *Chem. Rev.*, 2016, **116**, 3328–3435.
11 D. Wang, Q. Li, M. Li, Z. Du and Y. Fu, *Curr. Org. Chem.*, 2021, **25**, 1298–1320.
12 J. Rae, J. Frey, S. Jerhaoui, S. Choppin, J. Wencel-Delord and F. Colobert, *ACS Catal.*, 2018, **8**, 2805–2809.
13 X. Peng, A. Rahim, W. Peng, F. Jiang, Z. Gu and S. Wen, *Chem. Rev.*, 2023, **123**, 1364–1416.
14 K. Zhao, L. Duan, S. Xu, J. Jiang, Y. Fu and Z. Gu, *Chem*, 2018, **4**, 599–612.
15 K. Wang and W. Kong, *Chin. J. Chem.*, 2018, **36**, 247–256.
16 Q. M. Kainz, C. D. Matier, A. Bartoszewicz, S. L. Zultanski, J. C. Peters and G. C. Fu, *Science*, 2016, **351**, 681–684.
17 A. Cabré, X. Verdaguer and A. Riera, *Chem. Rev.*, 2022, **122**, 269–339.
18 Y. Tian, L. Hu, Y.-Z. Wang, X. Zhang and Q. Yin, *Org. Chem. Front.*, 2021, **8**, 2328–2342.
19 J. F. Hartwig and L. M. Stanley, *Acc. Chem. Res.*, 2010, **43**, 1461–1475.
20 S. L. Rössler, D. A. Petrone and E. M. Carreira, *Acc. Chem. Res.*, 2019, **52**, 2657–2672.
21 J. L. Kennemur, R. Maji, M. J. Scharf and B. List, *Chem. Rev.*, 2021, **121**, 14649–14681.
22 H.-H. Li, X. Chen and S. Kramer, *Chem. Sci.*, 2023, **14**, 13278–13289.
23 B. Xu, Q. Wang, C. Fang, Z.-M. Zhang and J. Zhang, *Chem. Soc. Rev.*, 2024, **53**, 883–971.
24 M.-Y. Huang and S.-F. Zhu, *Chem. Catal.*, 2022, **2**, 3112–3139.
25 M.-L. Li, J.-H. Yu, Y.-H. Li, S.-F. Zhu and Q.-L. Zhou, *Science*, 2019, **366**, 990–994.
26 Z.-S. Liu, P.-P. Xie, Y. Hua, C. Wu, Y. Ma, J. Chen, H.-G. Cheng, X. Hong and Q. Zhou, *Chem*, 2021, **7**, 1917–1932.
27 L. Jin, Y. Li, Y. Mao, X.-B. He, Z. Lu, Q. Zhang and B.-F. Shi, *Nat. Commun.*, 2024, **15**, 4908.
28 C.-J. Lu, Q. Xu, J. Feng and R.-R. Liu, *Angew. Chem., Int. Ed.*, 2023, **62**, e202216863.
29 K. Rossen, P. J. Pye, A. Maliakal and R. P. Volante, *J. Org. Chem.*, 1997, **62**, 6462–6463.
30 M. Kreis, C. J. Friedmann and S. Bräse, *Chem. – Eur. J.*, 2005, **11**, 7387–7394.
31 J. Tagashira, D. Imao, T. Yamamoto, T. Ohta, I. Furukawa and Y. Ito, *Tetrahedron: Asymmetry*, 2005, **16**, 2307–2314.
32 S. Vyskočil, M. Smrcina and P. Kočovský, *Tetrahedron Lett.*, 1998, **39**, 9289–9292.
33 P. Ramírez-López, A. Ros, A. Romero-Arenas, J. Iglesias Sigüenza, R. Fernández and J. M. Lassaletta, *J. Am. Chem. Soc.*, 2016, **138**, 12053–12056.
34 A. Castrogiovanni, D. Lotter, F. R. Bissegger and C. Sparr, *Chem. – Eur. J.*, 2020, **26**, 9864–9868.
35 X. Wang, W.-G. Liu, L.-T. Liu, X.-D. Yang, S. Niu, C.-H. Tung, L.-Z. Wu and H. Cong, *Org. Lett.*, 2021, **23**, 5485–5490.
36 S. Tong, J.-T. Li, D.-D. Liang, Y.-E. Zhang, Q.-Y. Feng, X. Zhang, J. Zhu and M.-X. Wang, *J. Am. Chem. Soc.*, 2020, **142**, 14432–14436.
37 J. Wei, V. Gandon and Y. Zhu, *J. Am. Chem. Soc.*, 2023, **145**, 16796–16811.
38 K. Takenaka, N. Itoh and H. Sasai, *Org. Lett.*, 2009, **11**, 1483–1486.
39 L. Porosa and R. D. Viirre, *Tetrahedron Lett.*, 2009, **50**, 4170–4173.

40 O. Kitagawa, M. Takahashi, M. Yoshikawa and T. Taguchi, *J. Am. Chem. Soc.*, 2005, **127**, 3676–3677.
41 O. Kitagawa, M. Yoshikawa, H. Tanabe, T. Morita, M. Takahashi, Y. Dobashi and T. Taguchi, *J. Am. Chem. Soc.*, 2006, **128**, 12923–12931.
42 M. Takahashi, H. Tanabe, T. Nakamura, D. Kuribara, T. Yamazaki and O. Kitagawa, *Tetrahedron*, 2010, **66**, 288–296.
43 A. Nakazaki, K. Miyagawa, N. Miyata and T. Nishikawa, *Eur. J. Org. Chem.*, 2015, 4603–4606.
44 T. Hirata, I. Takahashi, Y. Suzuki, H. Yoshida, H. Hasegawa and O. Kitagawa, *J. Org. Chem.*, 2016, **81**, 318–323.
45 W. Wang, M. Jiang, J. Li, F. Wang, X.-X. Li, J. Zhao and X. Li, *J. Am. Chem. Soc.*, 2024, **146**, 16567–16580.
46 I. Takahashi, F. Morita, S. Kusagaya, H. Fukaya and O. Kitagawa, *Tetrahedron: Asymmetry*, 2012, **23**, 1657–1662.
47 J. S. Sweet, S. Rajkumar, P. Dingwall and P. C. Knipe, *Eur. J. Org. Chem.*, 2021, 3980–3985.
48 X. Pu, Y. Zhang, X. He, X. Zhang, L. Jiang, R. Cao, M. Kin Tse and L. Qiu, *Adv. Synth. Catal.*, 2023, **365**, 1152–1157.
49 P. Zhang, C.-Q. Guo, W. Yao, C.-J. Lu, Y. Li, R. S. Paton and R.-R. Liu, *ACS Catal.*, 2023, **13**, 7680–7690.
50 H. Li, K. M. Belyk, J. Yin, Q. Chen, A. Hyde, Y. Ji, S. Oliver, M. T. Tudge, L.-C. Campeau and K. R. Campos, *J. Am. Chem. Soc.*, 2015, **137**, 13728–13731.
51 P. Zhang, Q. Xu, X.-M. Wang, J. Feng, C.-J. Lu, Y. Li and R.-R. Liu, *Angew. Chem., Int. Ed.*, 2022, **61**, e202212101.
52 P. Zhang, X.-M. Wang, Q. Xu, C.-Q. Guo, P. Wang, C.-J. Lu and R.-R. Liu, *Angew. Chem., Int. Ed.*, 2021, **60**, 21718–21722.
53 F.-B. Ge, Q.-K. Yin, C.-J. Lu, X. Xuan, J. Feng and R.-R. Liu, *Chin. J. Chem.*, 2024, **42**, 711–718.
54 L. Dai, *Prog. Chem.*, 2018, **30**, 1295–1297.
55 D. Ma and Q. Cai, *Acc. Chem. Res.*, 2008, **41**, 1450–1460.
56 C. Sambiagio, S. P. Marsden, A. J. Blacker and P. C. McGowan, *Chem. Soc. Rev.*, 2014, **43**, 3525–3550.
57 X. Xie, Y. Chen and D. Ma, *J. Am. Chem. Soc.*, 2006, **128**, 16050–16051.
58 F. Zhou, J. Guo, J. Liu, K. Ding, S. Yu and Q. Cai, *J. Am. Chem. Soc.*, 2012, **134**, 14326–14329.
59 J. Liu, J. Yan, D. Qin and Q. Cai, *Synthesis*, 2014, 1917–1923.
60 F. Zhou, G.-J. Cheng, W. Yang, Y. Long, S. Zhang, Y.-D. Wu, X. Zhang and Q. Cai, *Angew. Chem., Int. Ed.*, 2014, **53**, 9555–9559.
61 W. Yang, Y. Long, S. Zhang, Y. Zeng and Q. Cai, *Org. Lett.*, 2013, **15**, 3598–3601.
62 Y. Long, J. Shi, H. Liang, Y. Zeng and Q. Cai, *Synthesis*, 2015, 2844–2850.
63 J. Liu, Y. Tian, J. Shi, S. Zhang and Q. Cai, *Angew. Chem., Int. Ed.*, 2015, **54**, 10917–10920.
64 K. Takenaka, M. Sako, S. Takatani and H. Sasai, *ARKIVOC*, 2015, **2**, 52–63.
65 N. He, Y. Huo, J. Liu, Y. Huang, S. Zhang and Q. Cai, *Org. Lett.*, 2015, **17**, 374–377.
66 Z. Deng, Y. Ouyang, Y. Ao and Q. Cai, *Acta Chim. Sin.*, 2021, **79**, 649–652.
67 X. Fan, X. Zhang, C. Li and Z. Gu, *ACS Catal.*, 2019, **9**, 2286–2291.
68 Y. Liu, Z. Wang, B. Guo and Q. Cai, *Tetrahedron Lett.*, 2016, **57**, 2379–2381.
69 Y. Kwon, A. J. Chinn, B. Kim and S. J. Miller, *Angew. Chem., Int. Ed.*, 2018, **57**, 6251–6255.
70 Z.-C. Wang, P.-P. Xie, Y. Xu, X. Hong and S.-L. Shi, *Angew. Chem., Int. Ed.*, 2021, **60**, 16077–16084.
71 D. M. T. Chan, K. L. Monaco, R.-P. Wang and M. P. Winters, *Tetrahedron Lett.*, 1998, **39**, 2933–2936.
72 D. A. Evans, J. L. Katz and T. R. West, *Tetrahedron Lett.*, 1998, **39**, 2937–2940.
73 P. Y. S. Lam, C. G. Clark, S. Saubern, J. Adams, M. P. Winters, D. M. T. Chan and A. Combs, *Tetrahedron Lett.*, 1998, **39**, 2941–2944.
74 M. J. West, J. W. B. Fyfe, J. C. Vantourout and A. J. B. Watson, *Chem. Rev.*, 2019, **119**, 12491–12523.
75 V. Thönnißen, J. Westphäling, I. L. Atodiresei and F. W. Patureau, *Chem. – Eur. J.*, 2024, **30**, e202304378.
76 M. Ishida, R. Adachi, K. Kobayashi, Y. Yamamoto, C. Kawahara, T. Yamada, H. Aoyama, K. Kanomata, S. Akai, P. Y. S. Lam, H. Sajiki and T. Ikawa, *Chem. Commun.*, 2024, **60**, 678–681.
77 A. Yoshimura and V. V. Zhdankin, *Chem. Rev.*, 2016, **116**, 3328–3435.
78 V. V. Zhdankin and P. J. Stang, *Chem. Rev.*, 2008, **108**, 5299–5358.
79 K. Zhao, L. Duan, S. Xu, J. Jiang, Y. Fu and Z. Gu, *Chem*, 2018, **4**, 599–612.
80 S. Xu, K. Zhao and Z. Gu, *Adv. Synth. Catal.*, 2018, **360**, 3877–3883.
81 X. Zhang, K. Zhao, N. Li, J. Yu, L.-Z. Gong and Z. Gu, *Angew. Chem., Int. Ed.*, 2020, **59**, 19899–19904.
82 Q. Li, M. Zhang, S. Zhan and Z. Gu, *Org. Lett.*, 2019, **21**, 6374–6377.
83 Z. Chao, M. Ma and Z. Gu, *Org. Lett.*, 2020, **22**, 6441–6446.
84 W. Guo, J. Gu and Z. Gu, *Org. Lett.*, 2020, **22**, 7622–7628.
85 F. Cheng, D.-S. Duan, L.-M. Jiang, B.-S. Li, J.-X. Wang, Y.-J. Zhou, H.-Y. Jiao, T. Wu, D.-Y. Zhu and S.-H. Wang, *Org. Lett.*, 2022, **24**, 1394–1399.
86 S. Yang, T. Zheng, L. Duan, X. Xue and Z. Gu, *Angew. Chem., Int. Ed.*, 2023, **62**, e202302749.
87 J. Frey, A. Malekafzali, I. Delso, S. Choppin, F. Colobert and J. Wencel-Delord, *Angew. Chem., Int. Ed.*, 2020, **59**, 8844–8848.
88 Y.-L. Li, C. Zhang, X. Jin, X.-L. Yu, Z. Wang, H.-Z. Zhang and W.-Q. Yang, *Synlett*, 2020, 1077–1082.
89 Z.-L. Li, G.-C. Fang, Q.-S. Gu and X.-Y. Liu, *Chem. Soc. Rev.*, 2020, **49**, 32–48.
90 T. Bauer, Y. Z. Hakim and P. Morawska, *Molecules*, 2023, **28**, 6252.
91 F. Wang, P. Chen and G. Liu, *Acc. Chem. Res.*, 2018, **51**, 2036–2046.
92 S. Mondal, F. Dumur, D. Gigmes, M. P. Sibi, M. P. Bertrand and M. Nechab, *Chem. Rev.*, 2022, **122**, 5842–5976.
93 H. Lee, J. M. Ahn, P. H. Oyala, C. Citek, H. Yin, G. C. Fu and J. C. Peters, *J. Am. Chem. Soc.*, 2022, **144**, 4114–4123.

94 C. Chen, J. C. Peters and G. C. Fu, *Nature*, 2021, **596**, 250–256.
95 H. Cho, H. Suematsu, P. H. Oyala, J. C. Peters and G. C. Fu, *J. Am. Chem. Soc.*, 2022, **144**, 4550–4558.
96 A. Bartoszewicz, C. D. Matier and G. C. Fu, *J. Am. Chem. Soc.*, 2019, **141**, 14864–14869.
97 Y.-F. Zhang, X.-Y. Dong, J.-T. Cheng, N.-Y. Yang, L.-L. Wang, F.-L. Wang, C. Luan, J. Liu, Z.-L. Li, Q.-S. Gu and X.-Y. Liu, *J. Am. Chem. Soc.*, 2021, **143**, 15413–15419.
98 J.-J. Chen, J.-Y. Zhang, J.-H. Fang, X.-Y. Du, H.-D. Xia, B. Cheng, N. Li, Z.-L. Yu, J.-Q. Bian, F.-L. Wang, J.-J. Zheng, W.-L. Liu, Q.-S. Gu, Z.-L. Li and X.-Y. Liu, *J. Am. Chem. Soc.*, 2023, **145**, 14686–14696.
99 J.-J. Zheng, W.-L. Liu, Q.-S. Gu, Z.-L. Li, J.-J. Chen and X.-Y. Liu, *Precis. Chem.*, 2023, **1**, 576–582.
100 X.-Y. Du, J.-H. Fang, J.-J. Chen, B. Shen, W.-L. Liu, J.-Y. Zhang, X.-M. Ye, N.-Y. Yang, Q.-S. Gu, Z.-L. Li, P. Yu and X.-Y. Liu, *J. Am. Chem. Soc.*, 2024, **146**, 9444–9454.
101 J.-J. Chen, J.-H. Fang, X.-Y. Du, J.-Y. Zhang, J.-Q. Bian, F.-L. Wang, C. Luan, W.-L. Liu, J.-R. Liu, X.-Y. Dong, Z.-L. Li, Q.-S. Gu, Z. Dong and X.-Y. Liu, *Nature*, 2023, **618**, 294–300.
102 G. Zuccarello, S. M. Batiste, H. Cho and G. C. Fu, *J. Am. Chem. Soc.*, 2023, **145**, 3330–3334.
103 Y.-F. Zhang, J.-H. Wang, N.-Y. Yang, Z. Chen, L.-L. Wang, Q.-S. Gu, Z.-L. Li and X.-Y. Liu, *Angew. Chem., Int. Ed.*, 2023, **62**, e202302983.